7 SCIENTIFIC HIGHLIGHT OF THE MONTH

Density Functional Studies of Molecular Magnets

Andrei V. Postnikov[1], Jens Kortus[2] and Mark R. Pederson[3]

[1] *Institute of Metal Physics, Russian Academy of Sciences, S. Kowalewskoj 18, Yekaterinburg 620219, Russia, and Osnabrück University – Department of Physics, D-49069 Osnabrück, Germany*

[2] *Max-Planck Institut für Festkörperforschung, Heisenbergstr. 1, D-70569 Stuttgart, Germany*

[3] *Center for Computational Materials Science, Naval Research Laboratory, Washington D.C. 20375, USA*

Abstract

After a general introduction into the field of molecular magnets the discussion focuses on a more specific discussion of their most important representative species, single-molecule magnets incorporating transition metal ions. We overview traditional model approaches for the phenomenological description of such systems and outline some ways used to parameterize the corresponding models from experiment and from first-principle calculations. The latter can be either multi-determinantal quantum chemical schemes or those based on the density functional theory. In particular we discuss Heisenberg exchange parameters and magnetic anisotropy constants. As a practical example, an introduction into problems and properties of some single-molecule magnets which gained much attention within last years, namely Mn_{12}-acetate, "Fe_8" and "V_{15}" systems, is given. This introduction into systems is followed by a critical comparison of calculation schemes based on the density functional theory that are particularly well suited for the study of molecular magnets. For the above systems we select some benchmark results, obtained by different methods. Finally, we outline our recent progress in the study of other single-molecule magnets, including six-membered "ferric wheels", "ferric stars" and 'Ni_4" molecules, which we studied with the use of first-principles methods SIESTA and NRLMOL.

1 Introduction

Following Olivier Kahn[7], who is considered by many as one of the founders of this research topic, *"Molecular magnetism deals with magnetic properties of isolated molecules and/or assemblies of molecules"* (Kahn, 1993). This definition is quite general and there has been recently more emphasis on the aspect of the rational design of molecular magnetic properties in the field (Verdaguer, 2001). Therefore, molecular magnetism is seen *"as a discipline which conceives, realizes, studies, and uses new molecular materials bearing new but predictable magnetic (and other) physical property"* (Linert and Verdaguer, 2003). At present it conveniently hosts many different activities involving methods of physical characterization of matter (optical, X-ray, Mössbauer and neutron spectroscopies, scanning microscopies) and attracts physical models of different degree of sophistication and abstraction. The progress in the field is clearly driven by advances in chemical synthesis of the materials and experiments. However, the combined efforts of physicists and material scientists, particularly theorists, inspires confidence for that such efforts are not only useful for explaining but also for computationally tuning the synthesis of new promising materials. At the moment, the theory dealing with first principles calculations tries to keep the pace with experiment but is still at the stage trying to reproduce the experimental data rather than leading experiment. However, there has been notable progress in the prediction of exchange interactions and magnetic anisotropy energies from density-functional theory during the last few years. In contrast to cases where magnetic exchange interactions follow the famous Goodenough-Kanamori rules (Goodenough, 1955, 1958; Kanamori, 1959), in the case of magnetic anisotropy, another crucial property of molecular magnets, we still have to await similarly clean general insights derived from theory, which could revolutionize the rational design of molecular nanomagnets.

This field of research is very attractive for first-principles microscopic simulations, because the crystal structure of new molecular magnets is well defined, reproducible and is made available rapidly. This is in sharp contrast to the situation in nanoparticle materials or in surface studies where the structure data are usually more ambiguous. Synthetic chemists and theorists performing *ab initio* simulations despite different skills already speak a common language when discussing chemical bonding or magnetic interactions.

Whereas the actual execution of first-principles calculations did not require any special development of basically new numerical schemes, certain difficulties present in and specific to this type of materials provide interesting challenges to computational methods. For example, there are generally a large number of atoms (often several hundreds) in the unit cell, virtual absence of useful crystalline symmetry, and very inhomogeneous spatial distribution of charge density, with "very dense" and "almost empty" regions. The overall progress on the methodological side of atomistic first-principle calculations include more efficient basis sets, new order-N algorithms, along with general augmentation of computational power and this helps to address molecular magnets at a the atomistic level. This task would have been too complicated a decade ago.

The number of materials brought into discussion as molecular magnets is considerable, and some systematics might be appropriate to define better the subject of our present discussion.

[7]Unfortunately for all of us O. Kahn died the 8th December 1999.

Generally, all materials containing organic building parts and spins associated with unpaired electron(s) fall into one or another category of molecular magnets. Possible classifications may depend on the origin of the unpaired electron(s), the resulting moment localization and mobility, the type of interaction between individual moments, or their spatial organization (weakly coupled molecular fragments; 1-, 2- or 3-dimensional connected structures). A well structured general overview of different classes of molecular magnetic materials can be found in (Molecule-based magnets, 2000).

Magnetic *molecules* contain one or more transition metal centers or rare-earth ions or just organic radicals which are locked at their lattice sites by a careful chemistry of surrounding organic fragments. We won't discuss purely organic magnets where spins are carried by free radicals, although such systems clearly belong to the topic of molecular magnetism, and ferromagnetic ordering with T_c of 35.5 K (Banister *et al.*, 1996) have been demonstrated in them. In the following we restrict ourselves to systems where the spins reside on $3d$ transition metal ions.

In particular we will concentrate on the so-called single molecule magnets (SMM) – see Sessoli *et al.* (1993), – which are often also called molecular nanomagnets. Such materials can often be crystallized, but interactions between the molecular entities remain weak, so that the magnetic behavior probed by experiments is often dominated by intramolecular effects. The discovery of a molecule containing 12 manganese ions $Mn_{12}O_{12}(CH_3COO)_{16}(H_2O)_4$ with a magnetic ground state of $S=10$ showing a magnetic hysteresis (Sessoli *et al.*, 1993) due to the properties of the single Mn_{12}-molecules have boosted interest in the field enormously. The observed hysteresis in molecular magnets is *not* due to re-magnetization of domains, as in conventional ferromagnets, but reflects the "magnetization tunneling" (Friedman *et al.*, 1996) between quantum states of different m, $-S \leq m \leq S$, of the total spin S of the molecule, as the external magnetic field realigns the degeneracies of different states. This process can only be observed because the relaxation time is very large compared to the measurement time. The relaxation of the magnetization becomes indeed very slow at low temperatures (of the order of several months at 2 K). A single molecule behaves like a single domain and is relatively independent on the magnetization of its neighboring molecules.

What is the present state of art, "figures of merit", perspectives etc. in the field of molecular magnets? The field is becoming rapidly too large to cover all aspects in a compact introduction. There is a number of recent good reviews by Barbara and Gunther (1999); Gatteschi and Sessoli (2003); Verdaguer (2001), along with special issues of journals and conference proceedings (Linert and Verdaguer, 2003; Molecule-based magnets, 2000) which help to access the situation. We single out just several promising directions:

- Single molecule units as "bits" for magnetic storage. The size of molecules of interest is about one order of magnitude smaller than presently accessible domains in magnetic layers, and further miniaturization of conventional domains will be prevented at some point by approaching the superparamagnetic limit. This problem doesn't arise for magnetic molecules, because the *intramolecular* magnetic order is set by the chemistry of a single molecule in question and not due to achieving certain critical size, or certain amount of magnetic atoms. In order to become practicable, this application needs molecules with net ferromagnetic (or ferrimagnetic) intramolecular ordering of sufficient strength (high

spin ground state S). The intramolecular magnetic interaction have to be strong enough to prevent decoupling of the spins within the molecule by thermal fluctuations, so that the single molecule effectively behaves like an atom with a giant spin S. Moreover, a high magnetic anisotropy is required, to prevent spontaneous re-orientation of the magnetization of the molecular unit, i.e. to increase its *blocking temperature*. The intrinsic magnetic anisotropy becomes the temperature-determining figure of merit. Weak interactions between adjacent molecules, a prerequisite for writing down magnetic bits independently in each molecule, are usually taken for granted. Potential candidates for such applications, albeit with properties not yet good enough for any real application, are represented by "Mn_{12}-acetate" and "Fe_8" molecules, both with S=10, to be discussed below.

- Working units for quantum computation. This requires a scheme to populate and manipulate excited states of a molecular magnet in a controllable way. Leuenberger and Loss (2001); Leuenberger *et al.* (2003) proposed a seemingly feasibly scheme of imposing a prepared electron spin resonance impulse to write in, transform, and read out the information on a quantum state in the multilevel system of, say, S=10, explicitly referring to two above mentioned systems, "Mn_{12}-acetate" and "Fe_8". A promising technique may make use of the abovementioned magnetization tunneling (Friedman *et al.*, 1996).

- Room-temperature molecule-based permanent magnets, very different in some aspects (solubility in various solvents, biocompatibility) from "conventional" (e.g. intermetallics-based) magnets, and possessing an additional advantage of exhibiting interesting combined magnetooptical and electrooptical properties. Many such systems are based on Prussian blue analogues (Ohkoshi and Hashimoto, 2002; Verdaguer *et al.*, 1999, 2002). Curie temperatures as large as 42 °C (Ferlay *et al.*, 1995), 53 °C (Verdaguer *et al.*, 1999) and 103 °C (Holmes and Girolami, 1999), have been achieved with V, Cr-based Prussian blue analogues. Although such systems can be investigated by first principles calculations without principal problems (see, e.g., Pederson *et al.*, 2002c) and despite the fact that they are generally recognized as molecular magnets, we leave them beyond the current discussion, because they are formed of extended metallorganic patterns Such three-dimensional connectivity is of course essential for obtaining substantial values of T_c.

- Systems which exhibit novel collective phenomena such as magnetism switching by light, temperature, pressure or other physical interactions. Molecules which exhibit spin-crossover behavior would for instance fall into that class. Many such systems are among Fe-binuclear complexes (Gaspar *et al.*, 2003; Ksenofontov *et al.*, 2001a,a). The spin-crossover effects (switching between high-spin and low-spin states in different combinations at two Fe centers) are usually discussed in terms of interplay between intramolecular and intermolecular magnetic interactions, the latter being smaller but not negligible.

2 Structures and properties of some single molecule magnets

Now, in order to make first contact with the materials we are discussing, we review basic structural properties of some examples of the most intensely investigated SMM. From here on we

will use Mn_{12}-ac as shorthand for the complete chemical formula $Mn_{12}O_{12}(CH_3COO)_{16}(H_2O)_4 \cdot 2$ $CH_3COOH \cdot 4$ - H_2O.[8] The Mn_{12}-ac was the first example which showed the slow magnetization relaxation characteristic for a single molecule magnet. This compound is probably the most investigated SMM and, along with the oxo-nuclear iron compound Fe_8, it has shown so far many manifestations of interesting magnetic behavior which keep the research in the field growing. We'll discuss the structure and magnetic properties of these two magnetic molecules in more detail, because one can look at them as kind of test cases the theory was able to explain. For a concise and basic introduction into the field of single molecule magnets we refer the reader to Barbara and Gunther (1999).

2.1 Mn_{12}-ac magnet

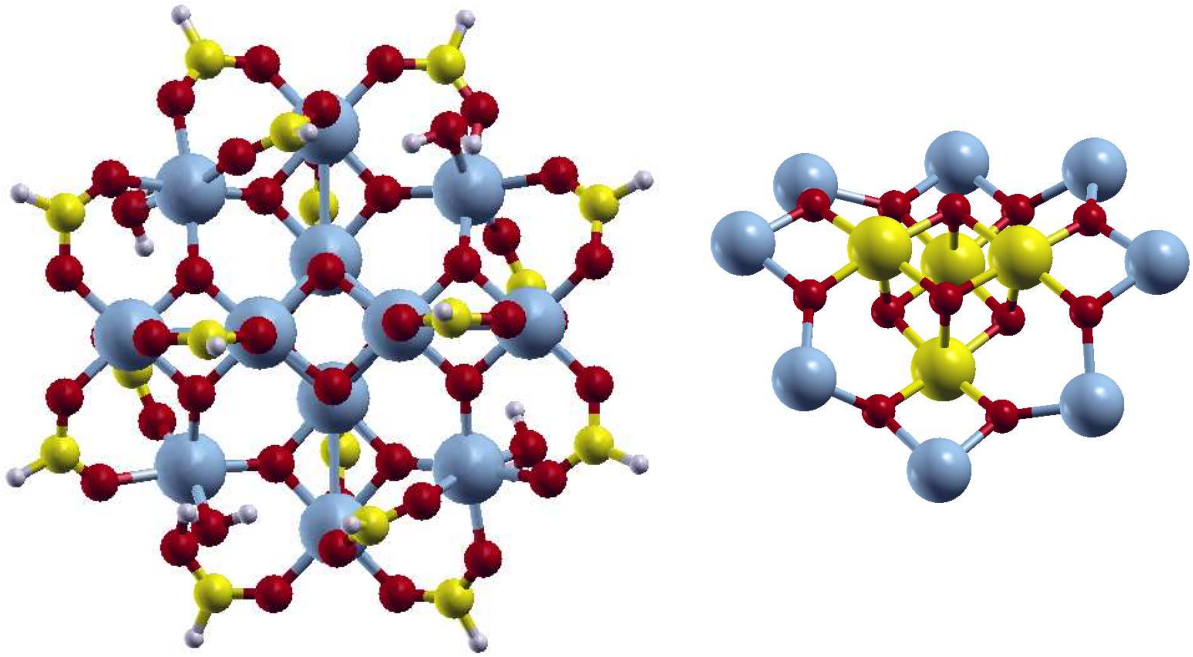

Figure 1: The ball and stick model of Mn_{12}-ac. Left panel: the entire molecule, with methyl groups replaced for clarity by hydrogen atoms (large balls are Mn atoms). Right panel: the magnetic core $Mn_{12}O_{12}$. Eight outer Mn ions have spins $s = 2$ ordered in parallel, four inner $s = 3/2$ are antiparallel to them, resulting in ferrimagnetic structure with total spin $S = 10$.

Mn_{12}-ac has been synthesized and reported in 1980 by Lis (1980). The molecular crystal has tetragonal symmetry with space group $I\overline{4}$, a single Mn_{12}-ac cluster in the crystal posses a S_4 symmetry. Figure 1 shows a ball and stick model of the molecular structure including only some organic ligands. No water of crystallization and acetic acid molecules are included, although they may play an important role, in particular for the process of tunneling of the magnetization. The manganese atoms are six-fold coordinated but show significant Jahn-Teller induced local

[8] There are now several modification of Mn_{12}-ac known, with different crystal structures, solvent molecules and water coordination – see Gatteschi and Sessoli (2003) for more information. Basically the inner structure of the molecule is always the same, and we'll uniformly refer to all these species as Mn_{12}-ac.

O_h symmetry lowering due to partially filled e_g shells on the outer sites. Right panel of Fig. 1 shows only the magnetic core, for better clarity. The inner four Mn atoms which are in the charge state Mn^{4+} ($s=3/2$) form, together with four O atoms, a (slightly distorted) cube. The eight outer Mn atoms are in the Mn^{3+} ($s=2$) charge state. The inner Mn ions are coupled antiferromagnetically to the outer ones, yielding a ferrimagnetic groundstate with a total spin $S = 8\times 2 - 4\times 3/2 = 10$. An evidence of the $S = 10$ ground state has been obtained from high field magnetization studies by Caneschi *et al.* (1991) which later has been confirmed by different experimental techniques, such as high field EPR (Barra *et al.*, 1997), high field magnetic torque measurements (Cornia *et al.*, 2000) or neutron scattering (Mirebeau *et al.*, 1999; Robinson *et al.*, 2000).

The (outer) Mn^{3+} ions are distinguishable from manganese atoms in different charge state by the elongated structure of the oxygen atom coordination octahedra or the corresponding oxygen-manganese bond lengths which are typical for Jahn-Teller distortions known in many Mn(III)-systems. This seems to be important for the magnetic anisotropy of the SMM (Gatteschi and Sessoli, 2003).

A surprising feature of the Mn_{12} clusters is that they remain intact in solution. This has been demonstrated by NMR measurements on several derivatives of the material (Eppley *et al.*, 1995). This remarkable finding clearly suggests that the observed magnetic properties have indeed an intramolecular origin. This is further supported by specific heat measurements which found no evidence for long range order in the material (Gomes *et al.*, 1998). Each magnetic molecule in the crystal is well separated from its neighbors by water and acetic acid molecules; Barbara and Gunther (1999) estimate the volume fraction of molecules in crystal to be merely 5%. The critical energy scale for the magnetic behavior is the magnetic anisotropy energy which is of the order of 60 K. The dipole-dipole interaction between molecules is of about 0.03 meV, or 0.35 K, so that one can safely discard it, for practical reasons and for setting up calculations.

2.2 Fe_8 magnet

The octanuclear iron(III) molecular magnet of the chemical formula $[Fe_8O_2(OH)_{12}(tacn)_6]^{8+}$, with tacn = 1,4,7-trizacyclononane ($C_6N_3H_{15}$), is often referred to as the Fe_8-cluster. The structure the Fe_8-molecular crystal, first synthesized by Wieghardt *et al.* (1984), is shown in Fig. 2. It is acentric $P1$ with $a=10.52$, $b=14.05$ and $c=15.00$Å, $\alpha=89.90°$, $\beta=109.65°$ and $\gamma=109.27°$.

The approximate D_2 symmetry observed in the molecule (Wieghardt *et al.*, 1984) is formally broken by the presence of halide atoms and waters of crystallization. The iron atoms form a structure which is often described as a butterfly. The central iron atoms are connected by oxo-hydroxo bridges to the four outer ones. The large spheres show the iron atoms, which are Fe(III) ions with a d^5 electron configuration. The two inner Fe(III) atoms are coordinated octahedrally to oxygen and the bridging hydroxy ligands. The outer iron atoms are also in octahedral coordination with the corresponding oxy and hydroxy ligands and nitrogen atoms of the tacn-rings. The organic tacn-rings are very important for stabilizing the magnetic core of the molecule because the three pairs of nitrogen dangling bonds complete a quasi six-fold environment for the Fe atoms. Two of the Fe(III) atoms have antiparallel spin projections than

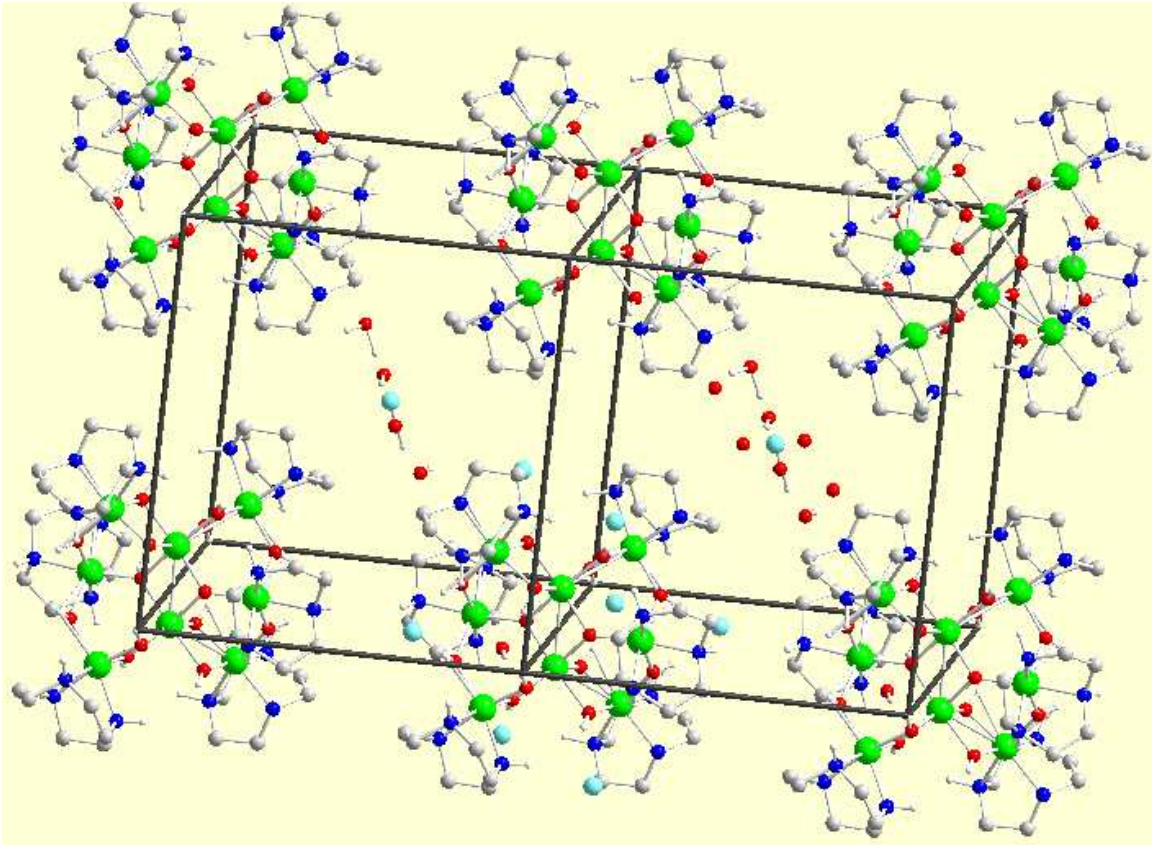

Figure 2: Repeated unit cells of the Fe_8 molecular crystal. Large green balls represent Fe.

the other six, so that the ferrimagnetic coupling of all eight results in the $S = 10$ spin ground state, as was directly proven by polarized neutron scattering measurements (Caciuffo *et al.*, 1998).

The tacn-rings separate the Fe_8-clusters in the crystal, resulting in negligible intermolecular dipole fields which are typically on the order of 0.05T (Wernsdorfer *et al.*, 1999). The resulting formal charge states are nominally Fe^{3+}, $(OH)^{-1}$ O^{-2}, and $tacn^0$, leading to a molecule with an overall formal charge state of +8, which must be compensated by negatively charged halide ions. Due to the lower symmetry as compared to Mn_{12}-ac, the Fe_8-cluster is allowed to have a transverse magnetic anisotropy, which is required in order to observe the quantum tunneling of the magnetization (QTM). This is because the transversal anisotropy is able to couple states with different m_s, that is a basic condition for "real" tunneling processes. In contrast, the tunneling in Mn_{12}-ac is often described as thermally, or phonon assisted, where dipolar and hyperfine interactions playing an important role (Gatteschi and Sessoli, 2003).

One of peculiar features of the Fe_8-cluster making it particularly interesting is that its magnetic relaxation becomes temperature independent below 0.36K, showing for the first time a pure quantum tunneling of the magnetization (Wernsdorfer *et al.*, 1999; Wernsdorfer and Sessoli, 1999). Further, the topological quenching of the tunnel splitting predicted by Garg (1993) has been observed in the form of a periodic dependence of the tunnel splitting on the magnetic field along the hard axis (Wernsdorfer and Sessoli, 1999).

2.3 V_{15} spin system

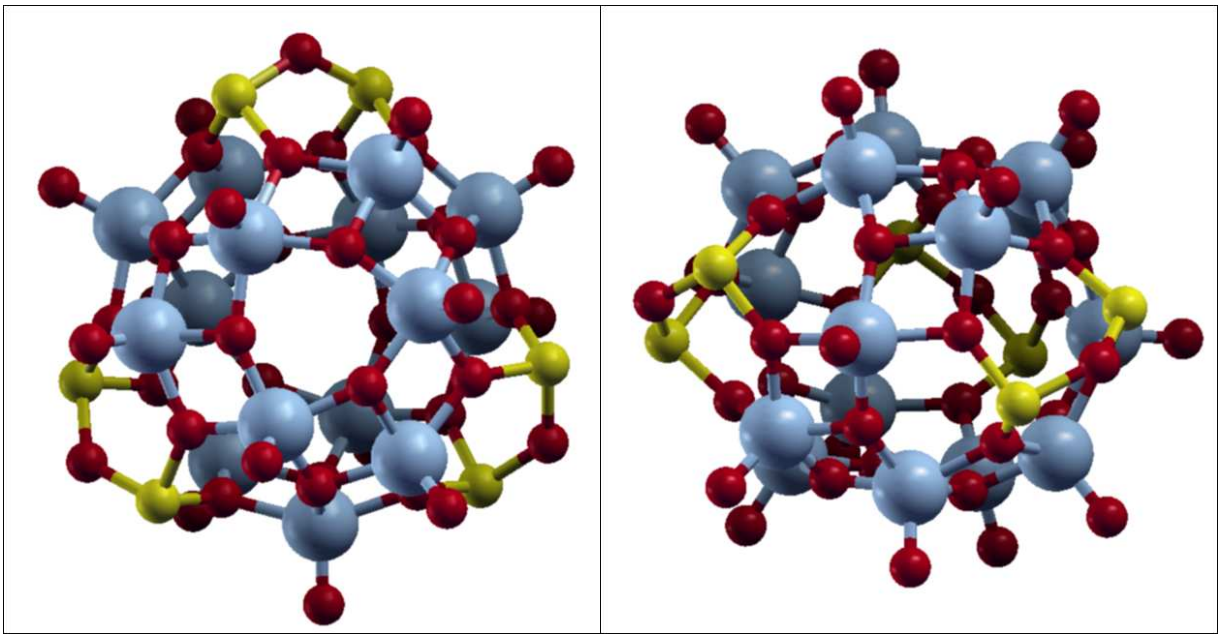

Figure 3: The top view (along the threefold axis, left panel) and the side view (right panel, note the sandwiched structure) to the ball and stick model of the V_{15} spin system. The large balls represent the 15 vanadium atoms. They all contain a single electron in the d-shell and couple in complicated ways to yield a total spin ground state configuration of $S = 1/2$.

The $K_6[V_{15}As_6O_{42}(H_2O)] \cdot 8H_2O$ molecular crystal was first synthesized by Müller and Döring (1988). The V_{15} molecule comprises spins s=1/2 at all vanadium atoms, which couple together to form a molecule with a total spin S=1/2 ground state. The weakly anisotropic V_{15} demonstrates quantum behavior, such as tunneling splitting of low lying spin states, and is an attractive model system for the study of mesoscopic quantum coherence and processes which destroy it. An understanding of such processes may be of interest for the field of quantum computing. V_{15} has a crystallographically imposed trigonal symmetry with three sets of inequivalent vanadium atoms (Gatteschi *et al.*, 1991). They form two hexagonal layers and an inner triangular layer sandwiched in between. The vanadium atoms are hold in place by oxygens and arsenic atoms so that the complete cluster forms a ball-, or cage-like structure. The empty space inside the cavity is often filled by a randomly oriented water molecule which strictly speaking would formally break the trigonal symmetry.

The unit cell contains two V_{15} clusters and is large enough so that dipolar interactions between them are negligible. Between 20K and 100K the effective paramagnetic moment is 3 μ_B, as for three independent spins, and below 0.5K it changes to the $S = 1/2$ ground state. The experimental results were interpreted with antiferromagnetic interactions between all vanadium atoms (Gatteschi *et al.*, 1991). In order to explain the magnetic behavior, a complicated spin Hamiltonian with many different exchange parameters J_{ij} (as indicated in Figure 4) is required (Kortus *et al.*, 2001a).

Due to the layered structure and the trigonal axis one expects that the V_{15} cluster will show interesting magnetic properties, such as a canted non-collinear magnetic ground state. Calcula-

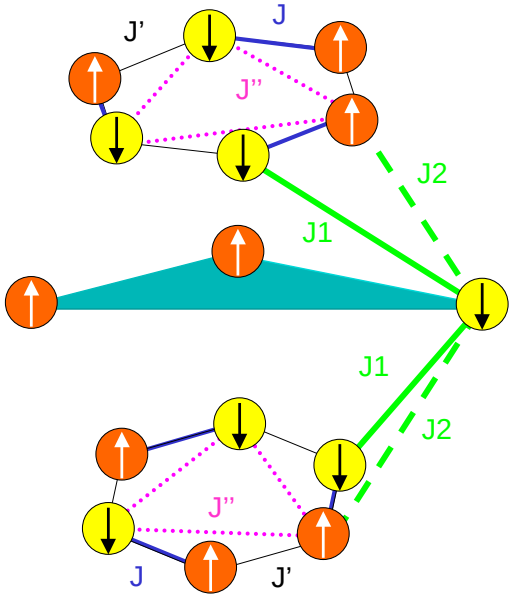

Figure 4: The scheme of different exchange coupling J_{ij} between 15 vanadium atoms needed for the description of the magnetic behavior of that compound. The spin configuration shown is that with the total spin $S=1/2$, corresponding to the lowest-energy DFT Ising spin configuration.

tions on such correlated systems present a challenge to mean-field frameworks such as density-functional theory, because it is often not possible to construct a single collinear reference state which preserves the inherent symmetry of the system and has the correct spin quantum numbers.

3 Magnetic interactions

A rather complicated and subtle subject that appears often in the discussion of experiments and theory of molecular magnets is that of interatomic magnetic interactions. We begin by introducing a consistent conceptual framework for the following discussion. Later on, we outline several calculation approaches which yielded valuable contribution in the understanding of molecular magnets, and list selected numerical results in their comparison. We conclude by presenting and discussing our new results on several molecular magnet systems of actual interest, that helps to grasp several typical features of electronic structure of this class of materials.

All discussion of magnetic interaction parameters makes sense only in the reference to a particular physical model which in general does not *explain* but *describes* mathematical relations between observables. In particular, the specific character of interaction between spins is not immediately available from calculation nor from experimental measurements. A directly measurable experimental information, like temperature or field dependency of magnetization or magnetic susceptibility, might be more or less satisfactorily fitted on the predictions of a certain model, yielding the values of interaction parameters in the sense of this particular model only. On their side, the first-principles calculations provide the spectrum of eigenvalues, or compare total energy in different magnetic configurations, and derive the estimates of interaction parameters from fitting these data, again, to a particular physical model. Therefore one should be

careful in comparing "measured" and "calculated" interaction parameters: they are accessed indirectly and from different starting points, hence their agreement may be accidental, and the source of disagreement not immediately obvious.

3.1 Spin Hamiltonians

The mechanisms of interaction do normally include, as the presumably leading term, the Heisenberg Hamiltonian

$$\mathcal{H} = -2\sum_{i>j} J_{ij}\mathbf{S}_i\mathbf{S}_j\,, \tag{2}$$

with the summation indicates that each pair of spins $\mathbf{S}_i$, $\mathbf{S}_j$ is counted only once. As only the relative orientation of both spins matters, this interaction is isotropic. The dependence on absolute spin orientation, i.e. with respect to the crystal lattice, can be brought in via a modification of the Heisenberg model taking into account anisotropy:

$$\mathcal{H} = -2\sum_{i>j} J_{ij}\left[S_i^z S_j^z + \gamma(S_i^x S_j^x + S_i^y S_j^y)\right]\,. \tag{3}$$

This form of interaction recovers the conventional Heisenberg model in case of γ=1, reduces to the Ising model for γ=0, or to the 2-dimensional interaction for $\gamma \gg 1$. Further on, the single-spin anisotropy can be included, and the Zeeman term added, yielding

$$\mathcal{H} = -2\sum_{i>j} J_{ij}(\mathbf{S}_i\mathbf{S}_j) - D\sum_i(\mathbf{e}_i\mathbf{S}_i)^2 - g\mu_{\mathrm{B}}\sum_i \mathbf{B}\,\mathbf{S}_i\,. \tag{4}$$

The single-spin anisotropy term may lack some of the true physics. It is scaled with its corresponding constant D and depends on the orientation of each spin $\mathbf{S}_i$ relative to a reasonably chosen fixed direction in space $\mathbf{e}_i$; the Zeeman term scales with the external magnetic field B, for the chosen value of the g factor.

It should be noted that the definition of the Heisenberg Hamiltonian in different works differs sometimes in the sign and in the presence of prefactor 2, that must be taken into account when comparing different sets of extracted parameters. The notation as above corresponds to $J > 0$ for ferromagnetic coupling.

A sophistication of such model spin Hamiltonian can be further enhanced by introducing additional parameters, i.e., distinguishing between random (varying from site to site) and constant (global) magnetic anisotropy, yielding the appearance of distinct D parameters in Eq. (4). Moreover, higher-order terms in isotropic interaction (biquadratic exchange, etc.), as well as from antisymmetric Dzyaloshinsky-Moriya spin exchange

$$\mathcal{H}_{\mathrm{DM}} = \sum_{i>j} \mathbf{D}_{ij}\cdot[\mathbf{S}_i\times\mathbf{S}_j]\,, \tag{5}$$

can be introduced. This might be necessary to grasp an essential physics, but makes the extraction of parameters, usually from a limited set of experimental data, more ambiguous, leading to a problem of over-parameterization.

The advantage of *ab initio* approaches to the extraction of interaction parameters is that certain mechanisms of interaction can be switched on and off in a fully controllable way. Thus,

all anisotropy terms may only have effect if the spin-orbit interaction is explicitly present in the calculation. The non-collinear orientation of individual spins can sometimes be arbitrarily chosen, and at least different settings of "up" and "down" configurations of spins with respect to a global quantization axis are normally available in any calculation scheme, so that angles between spins become in one or another way directly accessible.

The experiment does not allow such grade of control on the microscopic level; the magnetic field and temperature are eventually the only tunable parameters, and the availability of good-quality oriented monocrystalline samples is not a rule. Microscopic techniques include some (few) spectroscopic studies and (exclusively for Fe-based magnets) Mössbauer effect measurements; which are able, to some extent, to probe charge and spin state of an ion in question.

3.2 Relation to experiment

Once the spin Hamiltonian is agreed on, it can be, at least in principle, diagonalized, and its eigenvalues E_n determine the partition function and all thermodynamic properties in their dependency on magnetic field B and the temperature. Specifically, the molar magnetization is

$$M_{\mathrm{mol}} = -N_{\mathrm{A}} \frac{\sum\limits_n \partial E_n/\partial B \exp(-E_n/kT)}{\sum\limits_n \exp(-E_n/kT)} \tag{6}$$

(N_{A} is the Avogadro number), and the zero-field molar magnetic susceptibility, taking into account the dependence of eigenvalues E_n on the homogeneous magnetic field B_z up to the second order

$$E_n = W_n^{(0)} + B_z W_n^{(1)} + B_z^2 W_n^{(2)} + \dots \,, \tag{7}$$

yields

$$\chi_{\mathrm{mol}} = \mu_0 N_{\mathrm{A}} \frac{\sum\limits_n \left[(W_n^{(1)})^2/kT - 2W_n^{(2)} \right] \exp(-W_n^{(0)}/kT)}{\sum\limits_n \exp(-W_n^{(0)}/kT)} \,. \tag{8}$$

The evaluation of parameter values in the spin Hamiltonian proceeds by fitting thus obtained temperature (and/or magnetic field) dependencies to the measured data. The practical difficulty lies in the diagonalization of the Hamiltonian, whose dimension grows very rapidly with the number of spins and their S values.

A common conceptual difficulty is the necessity to choose between several sets of parameters which yield equally reasonable fit. An example of such ambiguity is given by Katsnelson *et al.* (1999) in fitting the model 8-spin Hamiltonian for Mn_{12}-ac to the neutron scattering data.

3.3 Relation to first-principles calculations

In first-principles calculations, one has the freedom to impose certain constraints (fix the magnitude or orientation of magnetization, modify the potential felt by certain electronic states, switch on or off the relativistic effects) and inspect the effect of this on the total energy. Moreover, one-electron eigenvalues and corresponding (Kohn-Sham, or Hartree-Fock) eigenfunctions are also available from a self-consistent calculation.

There are certain subtleties related to the assessment of exchange parameters from quantum chemistry (QC) and in DFT calculations.

In QC one deals with a multi-configurational scheme which allows to mix different spin configurations and to sort out energy eigenvalues corresponding to different total spin values. For two interacting spins $\mathbf{S}_1$, $\mathbf{S}_2$ summing up to $\mathbf{S}' = \mathbf{S}_1 + \mathbf{S}_2$ one gets

$$2\mathbf{S}_1\mathbf{S}_2 = \mathbf{S}'^2 - \mathbf{S}_1^2 - \mathbf{S}_2^2 \,,$$

with eigenvalues $[S'(S'+1) - S_1(S_1+1) - S_2(S_2+1)]$. For a textbook example $S_1 = \frac{1}{2}$, $S_2 = \frac{1}{2}$ this yields a singlet ($S' = 0$) and a triplet ($S' = 1$) states. The corresponding eigenvalues of the Heisenberg Hamiltonian must be then $3/2J$ and $-1/2J$, correspondingly.

Indeed, the basis functions in an *ab initio* calculation are normally pure spin states. In the basis of spin functions $|m_{S_1} m_{S_2}\rangle$, for the case $S_1 = \frac{1}{2}$, $S_2 = \frac{1}{2}$ the Heisenberg Hamiltonian takes the form:

$m_{S_1} m_{S_2}$	$\left\vert \frac{1}{2}\ \frac{1}{2}\right\rangle$	$\left\vert -\frac{1}{2}\ \frac{1}{2}\right\rangle$	$\left\vert \frac{1}{2}\ -\frac{1}{2}\right\rangle$	$\left\vert -\frac{1}{2}\ -\frac{1}{2}\right\rangle$
$\left\vert \frac{1}{2}\ \frac{1}{2}\right\rangle$	$-J/2$			
$\left\vert -\frac{1}{2}\ \frac{1}{2}\right\rangle$		$J/2$	$-J$	
$\left\vert \frac{1}{2}\ -\frac{1}{2}\right\rangle$		$-J$	$J/2$	
$\left\vert -\frac{1}{2}\ -\frac{1}{2}\right\rangle$				$-J/2$

(9)

The diagonalization of (9) is achieved by a basis transformation which mixes different m_S values:

$$\begin{array}{ll} \frac{1}{\sqrt{2}}\left(\left\vert \frac{1}{2}\ -\frac{1}{2}\right\rangle - \left\vert -\frac{1}{2}\ \frac{1}{2}\right\rangle \right) & \text{(singlet)} \quad S = 0 \quad E = \frac{3}{2}J \,; \\ \left\vert \frac{1}{2}\ \frac{1}{2}\right\rangle & \\ \frac{1}{\sqrt{2}}\left(\left\vert \frac{1}{2}\ -\frac{1}{2}\right\rangle + \left\vert -\frac{1}{2}\ \frac{1}{2}\right\rangle \right) & \text{(triplet)} \quad S = 1 \quad E = -\frac{1}{2}J \,. \\ \left\vert -\frac{1}{2}\ -\frac{1}{2}\right\rangle & \end{array}$$

(10)

In a QC (multi-determinantal) calculation, eigenvalues of singlet and triplet states, E_{S} and E_{T} correspondingly, are immediately accessible. This allows the (formal yet unambiguous) mapping of a first-principles result onto the Heisenberg model:

$$E_{\mathrm{S}} - E_{\mathrm{T}} = 2J \,. \tag{11}$$

The case $S_{1,2} = \frac{1}{2}$ corresponds to, e.g., two interacting Cu^{2+} ions. Other ions from the $3d$ row yield more rich system of eigenvalues – for instance, $S_{1,2} = 1$ (two Ni^{2+} ions) produces a quintet level E_{Q} beyond singlet and triplet, with the energy separation

$$E_{\mathrm{S}} - E_{\mathrm{Q}} = 6J \,. \tag{12}$$

Whether both equations (11) and Eq. (12) can be satisfied by the same J is a measure of validity of the Heisenberg model.

In a DFT calculation, the eigenvalues of multi-determinantal states are not available, and one must rely either on Kohn-Sham eigenvectors or on total energies in specially prepared symmetry-breaking metastable states, subject to different constraints with respect to spin states of a system. In practice, one can try ferromagnetic (FM) or antiferromagnetic (AFM) configurations of two spins, or impose the fixed spin moment (FSM) scheme, first introduced by Schwarz and

Mohn (1984). The total energy in different spin configurations relates *not* to eigenvectors but to diagonal elements of, e.g., the Hamiltonian $\mathcal{H}$ of (9):

$$\begin{aligned} E_{\rm FM} &= \left\langle \frac{1}{2}\,\frac{1}{2}\right| \mathcal{H} \left|\frac{1}{2}\,\frac{1}{2}\right\rangle = -\frac{1}{2}J\,, \\ E_{\rm AFM} &= \left\langle -\frac{1}{2}\,\frac{1}{2}\right| \mathcal{H} \left|-\frac{1}{2}\,\frac{1}{2}\right\rangle = \frac{1}{2}J\,, \end{aligned} \tag{13}$$

hence

$$E_{\rm AFM} - E_{\rm FM} = J \tag{14}$$

for the above case of $S_{1,2} = \frac{1}{2}$. This is a valid representation for J provided the Heisenberg model itself remains valid throughout the path from FM to AFM state. The latter formula can be approximated using the concept of magnetic transition state (Gubanov and Ellis, 1980). Generally, according to Slater, the shift in the DFT total energy ΔE due to a whatever change Δn_i in the occupation of certain orbitals is

$$\Delta E = \sum_i \Delta n_i \varepsilon_i^* + \mathcal{O}(\Delta n^3)\,, \tag{15}$$

where ε_i^* are Kohn-Sham eigenvalues obtained self-consistently with occupation numbers midway between initial and final states. For the flip from FM to AFM configuration,

$$E_{\rm FM} - E_{\rm AFM} \simeq \sum_i \left(n_{i\uparrow}^A - n_{i\downarrow}^A\right)\left(\varepsilon_{i\downarrow}^* - \varepsilon_{i\uparrow}^*\,,\right) \tag{16}$$

where $(n_{i\uparrow}^A - n_{i\downarrow}^A)$ is the magnetic moment (which gets inverted) in the orbital i, and the latter bracket is spin splitting (in energy) of the same orbital, calculated in the configuration with zero spin on atom A (transition state), i.e. induced fully via the interaction with the second spin. While being approximative, the magnetic transition state scheme might have a certain advantage of numerical stability over explicit comparison of large total energy values. Moreover, the result is available from a single calculation and offers a microscopical insight of how different orbitals are affected by magnetic interaction – the information which remains hidden in the total energy numbers. Being of use a number of times in the past (primarily for magnetic oxides), the method was recently applied for the analysis of exchange parameters in Mn_{12}-ac (Zeng *et al.*, 1999).

The validity of either "finite difference" scheme (14), or "differential" procedure (16) presumes that the mapping on the Heisenberg model makes sense, in the first place. However, with just two interacting spins we have no immediate criterion whether this is true. The applicability of the Heisenberg model would mean that the functional part of the interaction comes from the scalar product of two spin operators, with the parameter J_{ij} independent on $\mathbf{S}_i$ and $\mathbf{S}_j$. The mapping on the Heisenberg model may be less ambiguous if done as a limiting case of small deviations from a certain stationary state. The meaning of such deviations in the DFT might be some admixture to pure spin states (in the sense of local spin density functional), i.e., non-diagonal (in the spin space) form of density matrices. It allows a transparent quasi-classical interpretation in terms of non-collinear magnetic density varying from point to point in space – see Sandratskii (1998) for a review. If a pair of local magnetic moments can be reasonably identified in the calculation, and their small variations from the global magnetization

axis allowed, the counterparts in the Heisenberg model will be deviations of local exchange fields at two corresponding sites. Matching the leading terms in the angular dependence of interaction energy in the DFT and in the Heisenberg model yields the desired mapping. This line of arguing comes back at least to Oguchi *et al.* (1983) who extracted interaction parameters in simple $3d$ oxides from DFT calculations. Antropov *et al.* (1997); Liechtenstein *et al.* (1987, 1984) worked out closed expression for J_{ij} in a form consistent to spin-fluctuation theories[9] in terms of the elements of the Green's function. When using the final formulae, one should be careful to check whether they don't silently imply $S = 1/2$, and also examine the prefactor and sign which may be introduced differently. The following line of argument leads to the formula which has been applied in a number of calculations. If the total interaction energy of two quasi-classical spins is

$$E = J_{ij}\mathbf{S}_i\mathbf{S}_j\,, \tag{17}$$

its variation by deviating the spins by respective angles $\delta\varphi_i$, $\delta\varphi_j$ reads:

$$\delta^2 E = J_{ij}S^2\delta\varphi_i\delta\varphi_j\,. \tag{18}$$

In the attempt to cast a variation of DFT total energy in a comparable form, one can profit from the Andersen's local force theorem, which works here because we are interested in infinitesimal deviations from the ground state. An explicit derivation of the local force theorem in the desired form is given in an Appendix to the paper by Liechtenstein *et al.* (1987). In terms of the Green's function $\mathcal{G}$ and Kohn-Sham Hamiltonian $\mathcal{H}$ the first variation of the total energy reads

$$\delta E = -\frac{1}{\pi}\int^{\epsilon_\mathrm{F}} d\epsilon\ \mathrm{Im}\,\mathrm{Tr}\left(\delta\mathcal{H}\,\mathcal{G}\right) \tag{19}$$

(which can be shown to be zero), and the second variation

$$\delta^2 E = -\frac{1}{\pi}\int^{\epsilon_\mathrm{F}} d\epsilon\ \mathrm{Im}\,\mathrm{Tr}\left(\delta^2\mathcal{H}\,\mathcal{G} + \delta\mathcal{H}\,\mathcal{G}\,\delta\mathcal{H}\,\mathcal{G}\right)\,. \tag{20}$$

The variation of Kohn-Sham Hamiltonian can be explicitly related to rotations in spin space as

$$\delta\mathcal{H} = \frac{i}{2}\delta\varphi_i\left[\mathcal{H},\sigma\right]\,, \tag{21}$$

with the Hamiltonian composed of spin-dependent part at the site i, with $\Delta_i = V_i^{\uparrow} - V_i^{\downarrow}$ [a potential, in general, non-diagonal in (l,m)] and the rest $\mathcal{H}_0$:

$$\mathcal{H} = \frac{\Delta_i}{2}\begin{pmatrix} 1 & 0 \\ 0 & -1 \end{pmatrix} + \mathcal{H}_0\begin{pmatrix} 1 & 0 \\ 0 & 1 \end{pmatrix}\,. \tag{22}$$

This yields for the variation of $\mathcal{H}$

$$\delta\mathcal{H} = \frac{i}{2}\delta\varphi_x\ \Delta_i\begin{pmatrix} 0 & 1 \\ -1 & 0 \end{pmatrix} + \frac{1}{2}\delta\varphi_y\ \Delta_i\begin{pmatrix} 0 & 1 \\ 1 & 0 \end{pmatrix}\,. \tag{23}$$

Extracting from Eq. (20) the terms bilinear in $\delta\varphi_i$, recovering cite and spin indexes in the elements of the Green's function G_σ^{ij} and implying the summation in (l,m) yields

$$J_{ij} = -\frac{1}{2\pi}\mathrm{Im}\int^{\epsilon_F} d\epsilon\left(\Delta_i G_\uparrow^{ij}\Delta_j G_\downarrow^{ji} + \Delta_i G_\downarrow^{ij}\Delta_j G_\uparrow^{ji}\right)\,. \tag{24}$$

[9] with magnitude of spin varying, and attributed to J. Note therefore the difference in the definition of J_{ij} between these papers and Eq. (2).

This is the final formula for interaction between isolated spins in otherwise infinite and unperturbed environment. If one is interested in the interaction between two *sublattices* of periodically repeated atom types i and j, the Green function follows explicitly in terms of Kohn-Sham eigenfunctions $\psi^{ilm}_{n\mathbf{k}\sigma}$ and eigenvalues $\epsilon_{n\mathbf{k}\sigma}$

$$G^{ij}_{lm,l'm'}(\epsilon) = \sum_{\mathbf{k}n} \frac{\psi^{*ilm}_{n\mathbf{k}} \psi^{jl'm'}_{n\mathbf{k}}}{\epsilon - \epsilon_{n\mathbf{k}}} \tag{25}$$

and, using for the product of Green's functions

$$\frac{1}{(\epsilon - \epsilon_n)(\epsilon - \epsilon_{n'})} = \frac{1}{\epsilon_n - \epsilon_{n'}} \left(\frac{1}{\epsilon - \epsilon_n} - \frac{1}{\epsilon - \epsilon_{n'}} \right) , \tag{26}$$

the integration in energy over occupied states yields

$$J_{ij} = \sum_{\{m\}} \Delta^i_{mm'} \, \chi^{ij}_{mm'm''m'''} \, \Delta^j_{m''m'''} \tag{27}$$

in terms of non-local susceptibility, which depends on Kohn-Sham occupation numbers $n_{n\mathbf{k}\sigma}$,

$$\chi^{ij}_{mm'm''m'''} = \sum_{\mathbf{k}nn'} \frac{n_{n\mathbf{k}\uparrow} - n_{n'\mathbf{k}\downarrow}}{\epsilon_{n\mathbf{k}\uparrow} - \epsilon_{n'\mathbf{k}\downarrow}} \, \psi^{*ilm}_{n\mathbf{k}\uparrow} \psi^{ilm''}_{n\mathbf{k}\uparrow} \, \psi^{ilm'}_{n'\mathbf{k}\downarrow} \psi^{*ilm'''}_{n'\mathbf{k}\downarrow} , \tag{28}$$

– a formula probably first given by Liechtenstein *et al.* (1995) and used in a number of publications, notably by Boukhvalov *et al.* (2002) for Mn_{12}-ac. It should be understood that this formula describes interaction between two sublattices rather than two spins, and hence may give numbers very different from those by Eq. (27). The above derivation relates to $S = 1/2$, therefore the values reported for J_{ij} had to be rescaled according to actual interacting spins on, e.g., Mn atoms, a fact not always clearly stated in publications. Such scaling has been performed using the LDA (fractional) calculated values of magnetic moments, rather than nominal (integer) values.[10]

3.4 Spin-orbit coupling and magnetic anisotropy energy

As early as 1937 van Vleck pointed out that the magnetic anisotropy (MAE) arises mainly because of spin-orbit coupling and other relativistic terms in the Hamiltonian. Calculations of MAE on solids, layered structures and films have been carried out for many years using density-functional theory (Jansen, 1988, 1999; Schneider and Jansen, 2000; Shick *et al.*, 1998; Zhong *et al.*, 1991). Several problems associated with the accurate density-functional-based determination of MAE in the solid state have been identified. For example the role of incomplete orbital polarization has been shown to be one issue related to inaccuracies in the solid; other may be related to correlation effects beyond the mean-field treatment of correlations in the DFT.

Recently, Pederson and Khanna (1999b,c) have developed a method for accounting for second-order anisotropy energies. This method relies on a simple albeit exact method for spin-orbit coupling and a second-order perturbative treatment of the spin Hamiltonian to determine the dependence of the total energy on spin projection. The Cartesian representation of the spin-orbit term is used which is exact and also is more adaptable for multi-center systems:

$$U(\mathbf{r}, \mathbf{p}, \mathbf{S}) = -\frac{1}{2c^2} \mathbf{S} \cdot \mathbf{p} \times \nabla \mathbf{\Phi}(\mathbf{r}) \, . \tag{29}$$

[10] D. Boukhvalov, private communication.

Using single-particle wavefunctions expressed in terms of a basis set

$$\psi_{is}(\mathbf{r}) = \sum_{j,\sigma} C_{j\sigma}^{is} \phi_j(\mathbf{r}) \chi_\sigma, \tag{30}$$

where the $\phi_j(\mathbf{r})$ are the spatial functions and χ are spin functions, the matrix elements can be expressed as

$$\begin{aligned} U_{j,\sigma,k,\sigma'} &= \langle \phi_j \chi_\sigma \mid U(\mathbf{r},\mathbf{p},\mathbf{S}) \mid \phi_k \chi_{\sigma'} \rangle & (31) \\ &= -i \langle \phi_j \mid V_x \mid \phi_k \rangle \langle \chi_\sigma \mid S_x \mid \chi_{\sigma'} \rangle & (32) \end{aligned}$$

where the operator V_x is defined as

$$\langle \phi_j \mid V_x \mid \phi_k \rangle = \frac{1}{2c^2} \left(\left\langle \frac{d\phi_j}{dz} \middle| \Phi \middle| \frac{d\phi_k}{dy} \right\rangle - \left\langle \frac{d\phi_j}{dy} \middle| \Phi \middle| \frac{d\phi_k}{dz} \right\rangle \right). \tag{33}$$

In the above, $\Phi(\mathbf{r})$ is the Coulomb potential. Thus this treatment uses matrix elements of the Coulomb potential with partial derivatives of the basis functions, thereby avoiding the time consuming task of calculating the gradient of the Coulomb potential directly.

Here we generalize some of the derivations from uniaxial symmetry to an arbitrary one. The same definitions and lettering of the symbols is used as by Pederson and Khanna (1999c). In the absence of a magnetic field, the second-order perturbative change to the total energy of a system with arbitrary symmetry can be expressed as

$$\Delta_2 = \sum_{\sigma\sigma'} \sum_{ij} M_{ij}^{\sigma\sigma'} S_i^{\sigma\sigma'} S_j^{\sigma'\sigma}, \tag{34}$$

which is the generalization of Eq. (19) of Pederson and Khanna (1999c). In the above expression, σ sums over the spin degrees of freedom and i, j sums over all the coordinate labels, x, y, z respectively. The matrix elements $S_i^{\sigma\sigma'} = \langle \chi^\sigma | S_i | \chi^{\sigma'} \rangle$ implicitly depend on the axis of quantization. The matrix elements $M_{ij}^{\sigma\sigma'}$ are given by

$$M_{ij}^{\sigma\sigma'} = -\sum_{kl} \frac{\langle \phi_{l\sigma} | V_i | \phi_{k\sigma'} \rangle \langle \phi_{k\sigma'} | V_j | \phi_{l\sigma} \rangle}{\varepsilon_{l\sigma} - \varepsilon_{k\sigma'}}, \tag{35}$$

where $\phi_{l\sigma}$ are occupied and $\phi_{k\sigma'}$ and unoccupied states and ε's are the energy of the corresponding states.

The above equation can be rewritten in a part diagonal in the spin index plus the non-diagonal remainder according to:

$$\Delta_2 = \sum_{ij} \sum_{\sigma} M_{ij}^{\sigma\sigma} S_i^{\sigma\sigma} S_j^{\sigma\sigma} + \sum_{ij} \sum_{\sigma \neq \sigma'} M_{ij}^{\sigma\sigma'} S_i^{\sigma\sigma'} S_j^{\sigma'\sigma}. \tag{36}$$

Using the following relation for the expectation value of a spin operator in a closed shell molecule with excess majority spin electrons ΔN

$$\langle 1 | S_i | 1 \rangle = -\langle 2 | S_i | 2 \rangle = \frac{\langle S_i \rangle}{\Delta N}, \tag{37}$$

the first term of Eq. (36) can be expressed as

$$\sum_{ij} (M_{ij}^{11} + M_{ij}^{22}) \frac{\langle S_i \rangle \langle S_j \rangle}{(\Delta N)^2}. \tag{38}$$

With the help of

$$\begin{aligned}\langle 1|S_i|2\rangle\langle 2|S_j|1\rangle &= \langle 1|S_iS_j|1\rangle - \langle 1|S_i|1\rangle\langle 1|S_j|1\rangle \\ &= \langle 1|S_iS_j|1\rangle - \frac{\langle S_i\rangle\langle S_j\rangle}{(\Delta N)^2},\end{aligned} \tag{39}$$

and similar relation for $\langle 2|S_i|1\rangle\langle 1|S_j|2\rangle$, and a bit of algebra the second term of Eq. (36) becomes

$$\sum_{ij} -(M_{ij}^{12} + M_{ij}^{21})\frac{\langle S_i\rangle\langle S_j\rangle}{(\Delta N)^2} + \frac{1}{4}\sum_i M_{ii}^{12} + M_{ii}^{21} \ . \tag{40}$$

Therefore, the total second order shift Δ_2 together from Eq.(38) and Eq.(40) becomes

$$\begin{aligned}\Delta_2 &= \frac{1}{4}\sum_i M_{ii}^{12} + M_{ii}^{21} + \\ &\quad \sum_{ij}(M_{ij}^{11} + M_{ij}^{22} - M_{ij}^{12} - M_{ij}^{21})\frac{\langle S_i\rangle\langle S_j\rangle}{(\Delta N)^2}.\end{aligned} \tag{41}$$

As can be easily verified, the last equation gives the same result for uniaxial symmetry as Eq. (21) of Pederson and Khanna (1999c), where the Cartesian off-diagonal M_{ij} matrices vanish and $M_{xx}^{\sigma\sigma'} = M_{yy}^{\sigma\sigma'}$. For the derivation of the above expression of Δ_2 we did not assume any particular symmetry, therefore the resulting expression is general.

In the following, we overview the record of first-principles calculations on some SMM, outline a few typical problems and discuss the achieved results and remaining difficulties.

4 Requirements to a DFT computational scheme; working approaches and levels of accuracy

Physical questions which are of interest in the study of molecular magnets are not basically different from those encountered in the study of magnetism and electronic structure of, say, bulk solids, surfaces, of clusters from first principles in the DFT. One is interested in a description of the ground-state electronic structure and, as far as possible, of lowest excitations, in terms of Kohn-Sham eigenvalues and corresponding charge and spin density. It is advantageous to have access to sufficiently accurate total energies for comparing different competing charge or spin configurations; moreover, forces could be needed to perform conjugate-gradient structure optimization, or simulation of vibrations. These requirements are quite common in the practice of DFT calculations. The simulation of molecular magnets presents, however, certain technical difficulties which are not necessary typical for all DFT applications, and impose limitations both on the choice of calculation code for an efficient use and on the number of systems addressed so far in a first-principle simulations. These difficulties are:

1. Large number of atoms, up to several hundreds of atoms per repeated structural unit.

2. Low space group (or, point group) symmetry – or none at all, that does not allow the methods which use (l, m)-expansions in lattice harmonics (KKR, FLAPW) to profit from efficient block diagonalization.

3. Typically large size of a simulation box and, on the average, low density of atoms, that makes planewave methods with a global basis set cutoff inefficient.

4. The presence of transition-metal, or even rare earth, atoms with deep core states and, sometimes, with important semicore, along with the rest of predominantly light organic atoms. This might create difficulties for the use of norm-conserving pseudopotentials.

5. In tight-binding methods with fixed basis sets, specific problems may arise due to the need to tune and optimize the basis, as charge configurations and spatial distribution of density in molecular magnets may differ from those one is acquainted with in crystalline compounds.

6. The lack of energy dispersion (due to very week coupling between molecular units) and quite commonly a dense spectrum of nearly degenerate discrete states in the vicinity of HOMO-LUMO gap, which makes the self-consistency slowly convergent or even unstable.

Retrospectively, it seems understandable that larger number of calculations done so far employed one or another scheme using flexible tight-binding bases. Pseudopotential planewave calculations are not much represented, although one may expect an increase of their fraction, particularly with the use of ultrasoft pseudopotentials, in the future. Other all-electron methods (FLAPW) were used only for benchmark calculations on simplified systems. One can also anticipate a certain impact of basis-free, purely numerical approaches in the future.

In the following we critically compare several families of methods which played, or are expected to play, an important role in DFT calculations on molecular magnets, and emphasize several representative results.

4.1 Tight-binding linear muffin-tin orbital methods

The **tight-binding linear muffin-tin orbitals** (TBLMTO – Andersen and Jepsen, 1984; Andersen *et al.*, 1987; TBLMTO homepage) method has been used by the Ekaterinburg group for calculations of electronic structure and interaction parameters of Mn_{12}-ac (Boukhvalov *et al.*, 2002) and V_{15} (Boukhvalov *et al.*, 2003). The calculation method used in these works was indeed TB-LMTO and not the LMTO method in the less accurate "orthogonal approximation" (Gunnarsson *et al.*, 1983) as erroneously cited in these publications.[11] The calculation used real (tetragonal) structure of molecular crystal and periodic boundary conditions. The interatomic exchange parameters J were estimated along Eq. (27,28).

Having the advantage of compact and flexible (numerical and adjustable in the course of calculation) basis set, the LMTO method faces difficulties in the treatment of loosely packed structures, as it employs space filling by atomic spheres and/or "empty spheres" – in crystals with large and low-symmetric cavities, a cumbersome and ambiguous procedure. There are further drawbacks of LMTO for the treatment of molecular magnets. First, the method always employs periodic boundary conditions, so that molecular units must be posed either in their true (and very diffuse) crystalline arrangement, or – in order to simulate them as as isolated entities – with substantially

[11] D. Boukhvalov, private communication

enlarged lattice parameters. Second, the method has limitation of only one principal quantum number per l value in the basis set, i.e., $3p$ and $4p$ states cannot be simultaneously present in the valence band. These deficiencies are known to degrade delicate results of calculation, such as placement of some bands, or their dispersion in solids. Therefore one should access the quantitative results of these LMTO calculations with care. Possible indications of inferior numerical accuracy are the total magnetic moment of the Mn_{12}-ac system which is 19 μ_B in the LDA, at variance with experiment and other calculations (Pederson and Khanna, 1999a,b,c; Zeng *et al.*, 1999), yielding 20 μ_B, as well as the absence of HOMO-LUMO gap in both Mn_{12}-ac and V_{15}, again in variance with calculations by different methods. One should note, however, that the overall shape of local DOS is consistent with results of other calculations.

Boukhvalov *et al.* emphasize the importance of intraatomic correlation in the description of magnetic interactions and excitation spectra of Mn_{12}-ac and V_{15}. This might well make sense as evidenced by rich experience to this subject with manganites and vanadates, where the local coordination of transition metal ions and electronic structure are somehow similar to those in molecular magnets. The intraatomic correlation may be brought into the calculation by means of the LDA+U approach (Anisimov *et al.*, 1997), and depending on the *ad hoc* choice of average Coulomb parameter U. There are certain arguments for the choice of this parameter in the papers cited, U=4 eV for V_{15} and U=8 eV for Mn_{12}-ac. Not less important than the actual results with these parameter values are the trends with U varying, which have been reported for Mn_{12}-ac. One finds that as U changes from 4 to 6 to 8 eV, the exchange interaction parameters between four inner Mn atoms of the cubane core vary from 37 to 33 to 30 K (other Mn–Mn interaction constants, of the same order of magnitude, change in a similar manner). Moreover, local magnetic moments on all Mn atoms get slightly enhanced, and the band gap increases from 1.35 to 1.78 to 2.01 eV. This trends follow from a qualitatively transparent fact that higher U values deepen in energy the occupied $3d$ states and plunge the unoccupied, thus increasing the band gap. As the spin-flip excitations across the gap become more difficult, and they contribute to nonlocal susceptibilities (the denominator in Eq. (28) increases), this has an effect of reducing the interatomic exchange interaction. This mechanism will further be discussed in Section 5.

4.2 Gaussian-type orbital methods: NRLMOL

• The linear combination of atomic orbitals method with a basis of **Gaussian-type orbitals**, of which several "flavors" are known and have been in use.

This approach is "full-potential" one in the sense that no muffin-tin or atomic spheres geometry is imposed, and the spatial form of potential is fairly general. In particular the version implemented in the Naval Research Laboratory Molecular Orbital Library (NRLMOL) code (Jackson and Pederson, 1990; NRLMOL homepage; Pederson and Jackson, 1990) has been frequently used in calculations on molecular magnets.

The NRLMOL program package developed by Pederson, Jackson and Porezag is an all-electron Gaussian-type orbital implementation of DFT (Briley *et al.*, 1998; Jackson and Pederson, 1990; Pederson and Jackson, 1990, 1991; Pederson *et al.*, 1988; Pederson and Lin, 1987; Pederson *et al.*, 2000c; Porezag and Pederson, 1999, 1996; Quong *et al.*, 1993). It has been applied successfully to calculate the electronic and magnetic properties of several molecular nanomagnets (Baruah

and Pederson, 2002, 2003; Bobadova-Parvanova *et al.*, 2002; Kortus *et al.*, 2002a,b, 2001a,b; Kortus and Pederson, 2000; Kortus *et al.*, 2002c; Pederson *et al.*, 2002a; Pederson and Khanna, 1999a,b; Pederson *et al.*, 2000a, 2002b, 2000b). By including the spin-orbit coupling it is possible to calculate the magnetic anisotropy energy, which is a crucial parameter for understanding the magnetic behavior of SMM. The agreement between experiment and the result from the first-principles calculation is in many cases surprisingly good. Therefore it seems to be suitable to give some details on this particular numerical implementation.

The molecular orbitals were expanded as linear combinations of Gaussian functions centered at the atomic sites; multicenter integrals are evaluated numerically on a specially generated variational integration mesh – see Pederson and Jackson (1990) for details. An efficient parallelization (Pederson *et al.*, 2000c) makes all-electron calculations with more than hundred atoms feasible in affordable time, a prerequisite for useful applications in the domain of SMM. The problem of basis optimization, severe one in all methods employing localized and fixed basis functions, is solved in NRLMOL by tuning to the solutions of self-consistent isolated atoms (Porezag and Pederson, 1999).

Self-consistent potentials, obtained numerically, are least-square fitted to the sum of bare spherical Gaussians or Gaussian-screened $1/r$ potentials, in order to facilitate multicenter integrations.

Given the basis sets and the Gaussian-representation of the atomic potentials, it is possible to obtain very good insight into the class of multicenter integrands that need to be integrated, and this information is used to generate a numerical variational integration mesh (Pederson and Jackson, 1990) that allows to precisely determine integrals required for calculation of secular matrices, total energies and derivatives according to:

$$I = \int \mathrm{d}\mathbf{r} Q(\mathbf{r}) = \sum_i Q(\mathbf{r}_i)\Omega_i \,, \tag{42}$$

where Ω_i is the volume associated with point $\mathbf{r}_i$. Errors arising from the numerical integration can easily be checked and controlled by adjusting a few parameters which control the mesh construction. It should be emphasized that the Gaussian-screened potential are only used to optimize the numerical quadrature schemes used for mesh generation.

Once self-consistency is achieved the forces acting on each atom are determined from the Hellmann-Feynman-Pulay theorem (Feynman, 1939; Hellmann, 1937; Pulay, 1969). After obtaining all the forces acting on all the atoms a conjugate-gradient method, or other force-based algorithms, can be used to carry out geometry optimizations. Once the equilibrium geometry and Kohn-Sham wavefunctions is obtained, the properties available for the analysis include (beyond the standard set provided by any DFT package) polarizabilities, vibrational frequencies, infrared and Raman spectra and magnetic anisotropy energies.

For the $[Mn_4O_3Cl_4(O_2CCH_2CH_3)_3(NC_5H_5)_3]$ system, containing as its core a $Mn_3^{3+}Mn^{4+}$ pyramid and possessing a magnetic moment of 9 μ_B per unit (Mn^{3+} spins are anti-ferromagnetically coupled to Mn^{4+}), Park, Pederson and Bernstein (2003) calculated the properties related to dimerization. The Mn_4 units were presumed to couple antiferromagnetically, based on their unusual quantum tunneling properties (Wernsdorfer *et al.*, 2002), that was now confirmed in a calculation by NRLMOL (Park *et al.*, 2003c). A fit to the Ising model yields intraatomic exchange parameters of 44 K (ferromagnetic; Mn_3^{3+}–Mn^{3+}) and -152 K (antiferromagnetic;

Mn_3^{3+}–Mn^{4+}) – both overestimated by roughly a factor of two in comparison with experiment-derived values. The intermolecular coupling of merely -0.24 K is also twice larger than the experimental fit value. In addition to structure relaxation, Park *et al.* performed a calculation of vibration spectra with infrared and Raman intensities – the data not yet available from experiment but extremely important for identification and further characterization of this molecular magnet.

4.3 Numerical atom-centered basis functions : Siesta

The Siesta method and computational code (Siesta homepage; Soler *et al.*, 2002) also uses compact atom-centered basis functions, but (differently from NRLMOL) numerical ones with strict spatial confinement, as the most frequent choice. (Gaussian-type orbitals, or other fixed functions at the user's convenience, are equally available for the basis set). Due to strict confinement of basis functions, the program can make a clean distinction between cases of isolated fragment (molecule or cluster), "chain", "slab" or "crystal" cases (with periodic boundary conditions in one, two or three dimensions, correspondingly), and to correctly construct Madelung terms according to each case. Keeping trace on local neighborhood in the calculation of matrix elements, in combination with order-N facilities (see, e.g., Ordejón, 1998; Sánchez-Portal *et al.*, 1997), makes Siesta a great method for treating large low-coordination low-symmetry structures, as molecular magnets exactly are. In contrast to NRLMOL which determines the coulomb and exchange-correlation potentials analytically from the Gaussian representation of the wavefunctions, Siesta employs fast Fourier transform of the residual charge density (after subtraction of dominant atom-centered contributions) for the solution of the Poisson equation, that also yields high (and controllable) accuracy needed especially in the calculation of forces and optimization of structure. Moreover, for periodic systems (as molecular magnets generally are, in a crystalline state) the components of stress tensor are calculated, and can be used for simultaneous optimization of lattice parameters and internal coordinates subject to target pressure. Particularly important for magnetic systems is the option of treating "non-collinear" (i.e., not diagonal in the spin space) density matrix, that allows to simulate deviations of local magnetic moments from the global magnetic axis – for a recent application, see Postnikov *et al.* (2003b). Differently from two above discussed methods, Siesta is not all-electron one but employs norm-conserving pseudopotentials (Troullier and Martins, 1991, among other choices) and allows to apply the core correction after Louie *et al.* (1982). As the basis set is of localized functions and not planewaves, the use of hard pseudopotentials, like those of transition metals (also "small core", with semicore states attributed to the valence band) or oxygen, is not problematic. Siesta was designed in view of large distorted systems and dynamical simulations therein, so that properties of space group (or point group) symmetry are essentially lost. Therefore no special treatment of symmetrized molecular orbitals is provided.

As with other pseudopotential methods Siesta in its present version requires some care in choosing and testing pseudopotentials prior to calculation, and, moreover, in choosing basis orbitals. A certain freedom in the tuning of the latter is more matter of experience than of consistent control in a variational procedure (as is the case with planewave cutoff). Whereas being, as a rule, reasonably workable, such settings are difficult to consistently improve. More

insight in the problem of basis sets was provided by Sánchez-Portal *et al.* (1996) and Junquera *et al.* (2001).

The application of SIESTA to molecular magnets is relatively new. We outline some recent results below.

4.4 Discrete variational method

The **discrete variational method** (DVM) (Painter and Ellis, 1970; Rosen *et al.*, 1976), one of earliest DFT schemes to find applications in chemistry, seems to be potentially very well suited for the studies on molecular magnets. The method is all-electron one, it uses basis of numerical atomic orbitals, and the 3-dimensional integration over the space outside the spheres circumscribing core regions of each atom is done on a pseudorandom numerical grid. DVM was used in one of the first *ab initio* calculations of electronic structure of the Mn_{12}-acetate (Zeng *et al.*, 1999). Apart from discussing charge states, magnetic moments and local DOS of three distinct groups of Mn and O atoms in the molecule, which largely remained uncontested by subsequent calculations, Zeng *et al.* estimated Heisenberg exchange parameters in the magnetic transition state scheme (Gubanov and Ellis, 1980), an extension of Slater's original transition state *ansatz*, through a procedure outlined above in Sec. 3. Flipping the spin at one atom and detecting the shift of the $3d$-energy level on another one due to induced magnetic polarization helps to arrive at a system of equations where different interatomic exchange parameters are coupled. For the sake of simplicity and the clearness of analysis, only collective (non-symmetry-breaking) spin flips on all atoms belonging to each set of Mn atoms, – Mn(1) in the inner cubane, Mn(2) and Mn(3) in the peripheral region, see Fig. 1, – were allowed in the analysis of Zeng *et al.*. This means that four spins within each group always remained rigidly ferromagnetically coupled. It resulted in a system of three equations, whence the values of J_{12}, J_{23} and J_{13} could have been determined. The DFT results were explicitly fitted to the Heisenberg Hamiltonian of the form of Eq. (2). However, the parameters J_{11} etc., representing the coupling within each group, did not appear in the fit, because the spin excitations necessary to probe them, which would break the symmetry of the molecule, were not allowed. Their inclusion in an otherwise organized calculation could result in renormalization of exchange parameters.

The values of J_{12}, J_{23} and J_{13} are given in Table 1; they are all negative, i.e. indicate an AFM coupling (as could be expected due to a more-than-90° superexchange pathway through bridging oxygens), and hence frustration in accommodating three spin subsets.

4.5 Planwave methods

The use of **planewave** basis for calculation on molecules is, as was mentioned above, computationally inefficient, but technically feasible and, with sufficiently high cutoff, also ultimately accurate. Massobrio and Ruiz (2003) recently compared straightforward (from the total energy difference in low-spin and high-spin configuration) estimates of Heisenberg-model exchange parameters J for several Cu-based binuclear molecules: $Cu_2(CH_3COO)_4$, $[Cu_2(\mu\text{-}OH)_2(\text{bipyrimidine})_2](NO_3)_2{\cdot}4H_2O$ and $[(dpt)Cu(\mu\text{-}Cl)_2Cu(dpt)]Cl_2$ (dpt = dipropylenetriamine), using identical norm-conserving pseudopotentials and exchange-correlation scheme (among other,

Table 1: Electronic structure parameters of Mn_{12} from *ab initio* calculations.

Method	Magnetic moments (μ_B)			Heisenberg exchange parameters (K)		
	Mn(1)	Mn(2)	Mn(3)	J_{12}	J_{13}	J_{23}
DVM[a]	3.056	−3.889	−4.039	−136	−72	−102
NRLMOL[b]	2.57	−3.63	−3.58	−57	−41	−8
LMTO[c], U=4 eV	2.72	−3.44	−3.65	−53	−47	−19
LMTO[c], U=8 eV	2.92	−3.52	−3.84	−47	−26	−7

[a]Zeng *et al.* (1999); LDA.

[b]Pederson and Khanna (1999c); GGA; moments within a sphere of 2.5 Bohr. J values by Park *et al.* (2003b).

[c]Boukhvalov *et al.* (2002); LDA+U; moments within spheres of 2.7/2.8 Bohr (inner/outer Mn atoms).

differing options) as with Gaussian-type basis functions. The largest system consisted of 62 atoms, a moderate number by the standards of a calculation with localized basis functions. For the computational load with the planewave basis, however, it is the size of the simulation box that primarily matters. Here its linear size of 18.5 Å resulted in about $2.4{\cdot}10^6$ plane waves for the expansion of charge density and demanded hours of highly parallelized execution. The small values of J obtained in the plane-wave calculation (−518, −95 and +61 cm^{-1}, correspondingly) were of correct correct sign and order of magnitude in all cases, although deviations in absolute value, from experimental estimate and between different exchange-correlation flavors, were up to 50%.

5 Some recent developments

In the following we outline some recent results on relatively "new" molecular magnets, i.e. systems which have only become available during the last few years, For the study of their electronic characteristics several questions arose which our calculations attempted to clarify. "Ferric wheels" gained interest, not in the last place, because of their "esthetically rewarding" (Gatteschi and Pardi, 2003) shape. Two examples discussed below have an AFM ground state; consequently they might find applications related to quantum tunneling and quantum computing. Other structurally similar (although chemically different) examples include 3d ions (notably Mn) at larger distances, with magnetic interactions mediated by organic radical groups that lead to strong antiferromagnetic couplings of Mn ions. An example is the molecule $[Mn(hfac)_2(NITPh)]_6$ (hfac= hexafluoroacetylacetonate, NITPh= 2-phenyl-4,4,5,5-tetramethyl-4,5-dihydro-1H-imidazol-1-oxy-3-oxide), see Gatteschi and Pardi (2003) with a net spin of S=12. "Ferric stars" include a central 3d ion to which peripheric ions couple antiferromagnetically which results in a net spin value in the ground state. Due to their not-negligible magnetic anisotropy these systems look like possible prototypes for magnetic storage. Ni_4 is a seemingly simple magnetic molecule for which a fit of experimental data of magnetization vs. magnetic field to the

Heisenberg model fails quite dramatically, and possible reasons for deviation have been studied, with the help of first-principles calculations. Finally, we consider a two-nuclei model system with the aim to study the effect of intraatomic correlation ("Hubbard U") on the electronic structure and interatomic magnetic interactions in a more numerically accurate calculation than has yet been accomplished (for Mn_{12} by TB-LMTO, Boukhvalov *et al.*). In the most recent case the calculations have been performed with the FLAPW method (FLEUR homepage), for other systems – by methods using atom-centered localized basis functions, either SIESTA or NRLMOL.

5.1 "Ferric wheels"

Hexanuclear "ferric wheels" $M\mathrm{Fe}_6[\mathrm{N}(\mathrm{CH}_2\mathrm{CH}_2\mathrm{O})_3]_6\mathrm{Cl}$ (M = Li, Na, see Fig. 5), the systems to be discussed below, were synthesized at the Institut für Organische Chemie in Erlangen (Saalfrank *et al.*, 1997) and labeled as substances **4** and **3** in the latter publication. There exist a large family of ferric wheels with a different even number ($N = 6, 8, 10, 12, 18$) of iron atoms (Abbati *et al.*, 1997; Caneschi *et al.*, 1996, 1999, 1995; Pilawa *et al.*, 1997; Saalfrank *et al.*, 1997; Taft *et al.*, 1994; Taft and Lippard, 1990; Waldmann *et al.*, 2001, 1999; Watton *et al.*, 1997). Besides the ferric ones, there have been reports on wheels with other transition metal ions such as an eight membered Cr(III) wheel (van Slageren *et al.*, 2002), a Cu(II) (Lascialfari *et al.*, 2000; Rentschler *et al.*, 1996), a Co(II) (Brechin *et al.*, 2002), a Mn(II) (Abbati *et al.*, 1998) and a 24 membered Ni(II) wheel (Dearden *et al.*, 2001). The latter structure contains the largest so far number of transition metal ions in a wheel-like structure. Synthesis of odd-numbered magnetic wheels or necklesses appears to be a nontrivial task.

Fe atoms in these compounds are connected by oxo-bridges, that are reminescent of the 90° coupling of magnetic atoms in transition-metal oxides. The nearest coordination of the Fe atom is octahedral; two pairs of O ions form bridges to the neighboring Fe atoms on both sides; the fifth oxygen (referred to below as "apical") and the nitrogen ion are connected by the C_2H_4 group. The octahedra are slightly distorted, to accommodate the stiffness of oxo-bridges with the curvature of the molecular backbone. While the Fe–O–Fe angles differ slightly in the Li-centered and Na-centered wheels (101.1° and 103.3°, respectively), the structure of the two molecules is almost identical.

According to magnetization and torque measurements by Waldmann *et al.* (1999), these systems are characterized by S=5/2 on the Fe site, thus implying a highly ionized Fe(III) state. Moreover, a fit to the spin Hamiltonian of the Heisenberg model (2) yields the J values of -18 to -20 K for the Li-wheel (depending on sample and method) and -22.5 to -25 K for the Na-wheel, thus implying an AFM ground state (Waldmann *et al.*, 1999). X-ray photoelectron and X-ray emission spectroscopy studies (Postnikov *et al.*, 2003a) allowed for probing of the electronic structure in the valence band and on the Fe site, albeit without resolution in spin. Whereas the magnetic measurements data are by now well established, the spatially resolved distribution of magnetization was not yet accessed prior to the present calculation. Specifically, we compare the results of electronic structure calculations by two different methods within the DFT, SIESTA and NRLMOL (see the discussion on the methods in Sec. 4). In both cases we used the generalized gradient approximation after Perdew, Burke and Ernzerhof (1996). We emphasize that the most important difference between two methods, in what regards the present study, is that SIESTA

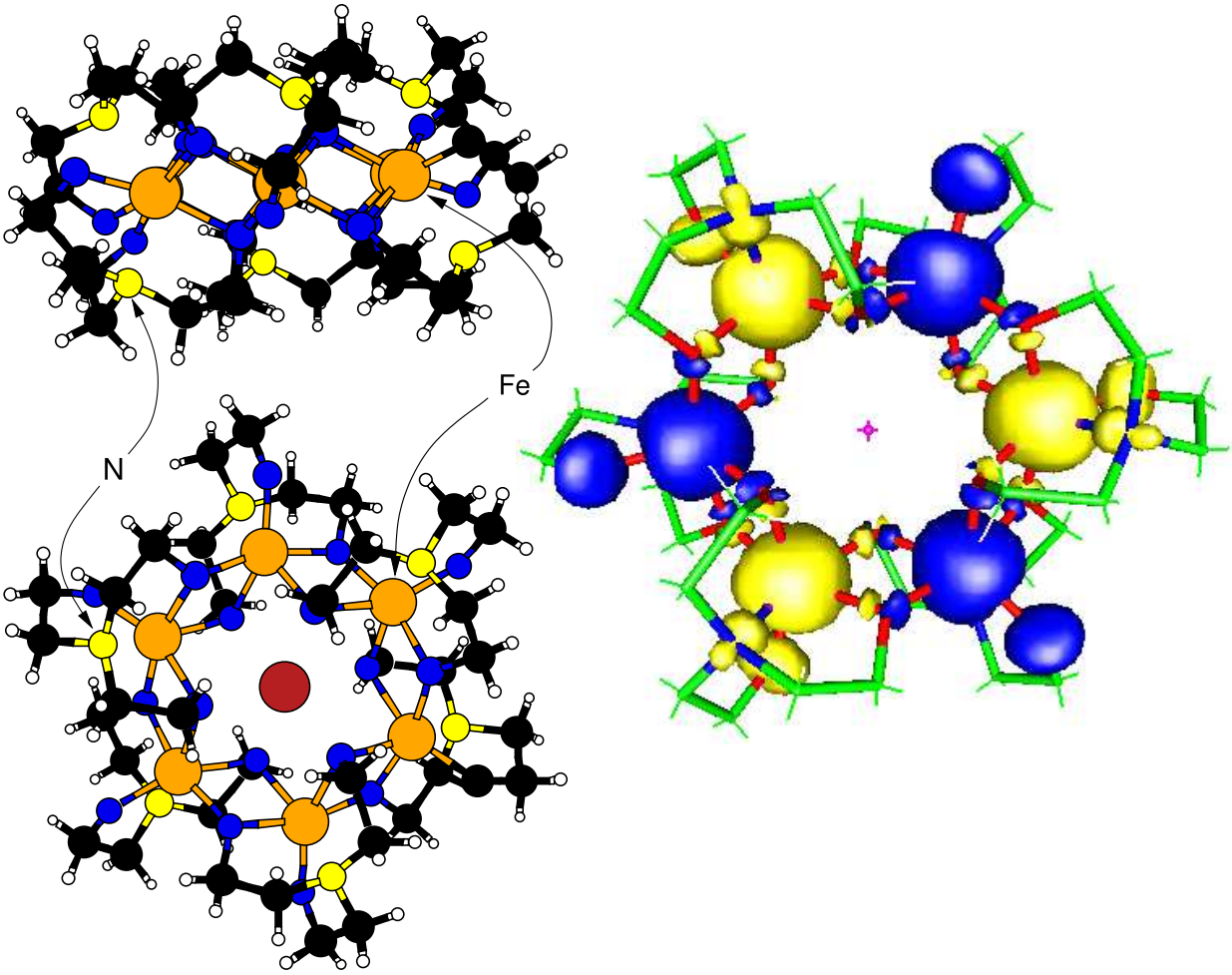

Figure 5: Structure and spin density distribution in "ferric wheel" molecules. Left panel: two views of the Li-centered molecule. The Li ion is in the middle of the ring; the distant Cl ion included in the simulation is not shown; the rest of (electrically neutral) solvent is neglected. Right panel: iso-surfaces correspond to $\pm 0.01 e/\text{Å}^3$, according to NRLMOL calculation (Postnikov *et al.*, 2003c). While most of the magnetic moment is localized at the Fe atoms, there is still some spin polarization on O and N.

uses norm-conserving pseudopotentials whereas NRLMOL implements an all-electron method. For an *ab initio* pseudopotential code such as SIESTA, benchmark calculations, based on the very accurate NRLMOL suite of codes, aid in accessing the accuracy of pseudo-potential based methods in some critical cases and/or for new systems.

We outline below the results obtained by SIESTA for the Li-centered molecule, and by NRLMOL – for the Na-centered one, as presented in more detail by Postnikov *et al.* (2003c). The NRLMOL treatment was restricted to the ground-state AFM configuration (alternating orientations of Fe magnetic moments over the ring); the SIESTA calculation addressed in addition different magnetic configurations, that allowed for the extraction of DFT-based exchange parameters.

Fig. 6 displays the partial densities of states (DOS) on Fe and its several neighbors in the AFM configuration, as calculated by both methods. The discrete levels of the energy spectra are weighted (with the charge density integrated over atom-centered spheres in NRLMOL, or

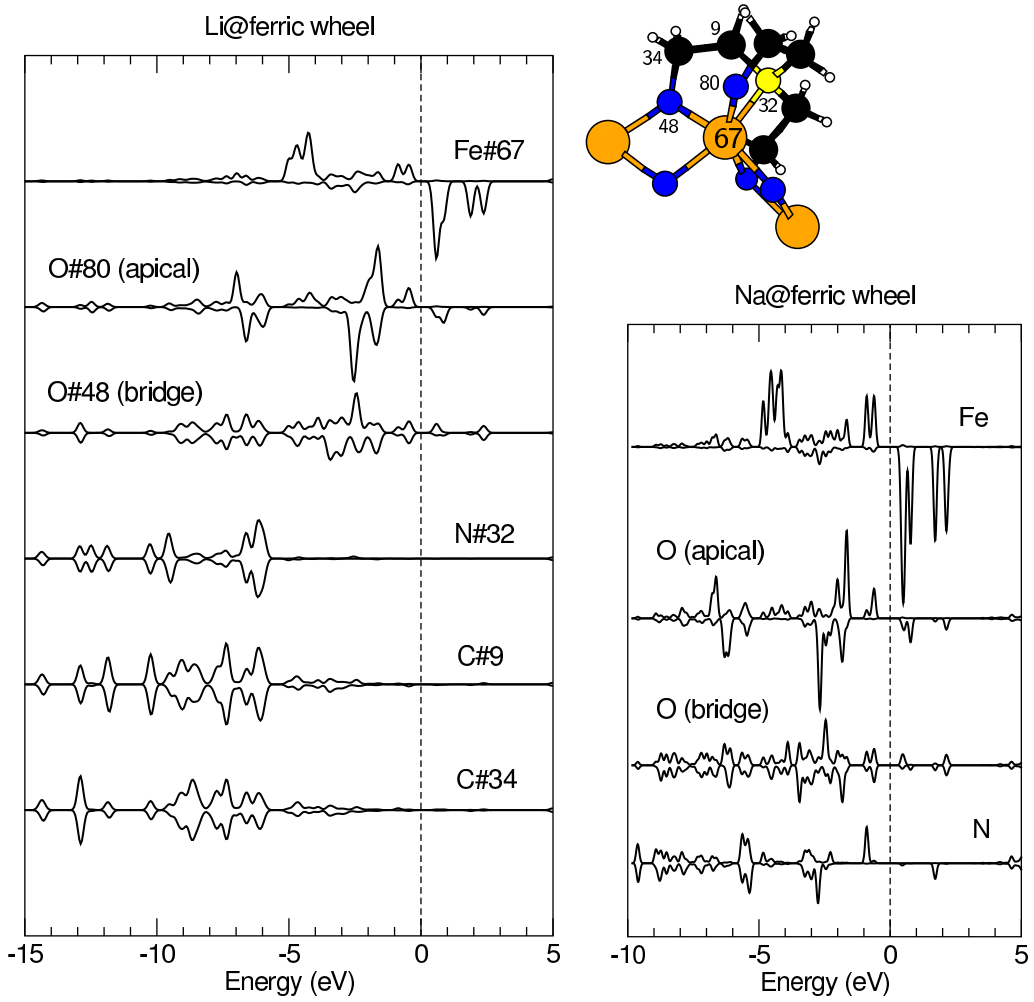

Figure 6: Atom- and spin-resolved partial densities of states as calculated for Li-centered molecule by SIESTA (left panel) and for Na-centered molecule by NRLMOL (right panel). The DOS at the Fe site is scaled down by a factor of 2 relative to other constituents. The numbering of atoms which are neighbors to the Fe atom is shown in the inset. See text for details on the calculation.

according to Mulliken population analysis in SIESTA), and broadened for presentational purposes with broadening parameter of 0.15 eV (SIESTA) and 0.14 eV (NRLMOL). The local moments corresponding to integrating such partial DOS over occupied states are given in Table 2. Both calculations give a consistent description of state densities at Fe and O sites, even though this property is rather loosely defined (and its calculation differently implemented in SIESTA and NRLMOL).

Notably, both methods find the local magnetic moments on Fe sites very close to 4 $\mu_{\rm B}$ and *not* to 5 $\mu_{\rm B}$ as is generally assumed, based on the above mentioned magnetization data. The maximal magnetization S=5/2 of the Fe atom corresponds to a Fe(III)-ion with in $3d^5_\uparrow d^0_\downarrow$ configuration. Our first-principles calculations suggest a somewhat different picture: the minority-spin DOS has a non-zero occupation due to the hybridization (chemical bonding) of Fe3d with O2p states. However, the magnetic polarization in the organic ligand which provides the octahedral coordination for the iron atoms, due to Fe is substantial, the most pronounced effect being on

the apical oxygen atom (which is not participating in the bonding to the next Fe neighbor). Taken together with the (smaller) polarization of the bridging oxygen atoms and magnetization at the nitrogen site, the distributed magnetic moment *per* Fe atom yields 5 μ_B, recovering the agreement with the magnetization results.

A clear visualization of the above discussed delocalized (or, rather, distributed) magnetic moment associated with the Fe atom comes from the map of spin density, obtained from the NRLMOL calculation (Fig. 5, right panel). One should take into account that the volume enclosed by the iso-surfaces is not directly correlated to the total moment at the site. One sees moreover an absence of magnetization on carbon and hydrogen sites. The fact that the magnetization is noticeable and changes its sign when passing through bridge oxygen atoms emphasizes the failure of methods depending the spherical averaging of atom-centered potentials.

An important consequence is that the charge state of iron is not Fe(III) but more close to Fe(II), according to our (JK+AP) calculations. Moreover, the distributed magnetic moment behaves like a rigid one, in a sense that it can be inverted, following a spin flip on a Fe site. This is illustrated by the analysis of other magnetic configurations, done with SIESTA (Postnikov *et al.*, 2003a). The local DOS does not change considerably when switching from AFM to FM configuration – only the HOMO/LUMO gap becomes less pronounced, and a slight ferromagnetic shift between the two spin bands appears.

For the sake of improving both the stability of convergence with SIESTA and for pinning down a particular spin configuration (FM, or with one or more Fe magnetic moments inverted), we applied the FSM scheme (Schwarz and Mohn, 1984) in the calculation. Imposing an (integer) spin moment per molecule fixes the number of electrons in two spin channels and removes a possibility of spin flips, which are a major source of numerical instability, as there are many nearly degenerate states in the vicinity of the Fermi level in the molecule (and no symmetry constraints on these states in SIESTA). The FSM procedure would normally split the common chemical potential in two separate ones, for majority- and minority-spin channels, that corresponds to an effective external magnetic field and hence to additional (Zeeman) term in the total energy, in analogy with Eq. (4). Since molecular magnets possess a HOMO-LUMO gap, the latter correction must only be considered if such gaps in two spin channels do not overlap. Fig. 7 shows the total energy values and energy gaps for FSM values of 30 μ_B (FM case), 20 and 10 μ_B (one and two local moments inverted, correspondingly); 0 (alternate-spin AFM case). A linear change

Table 2: Local magnetic moments M at Fe and its neighbors. NRLMOL results correspond to spin density integrated over sphere of radius R centered at corresponding atom; SIESTA values are due to Mulliken population analysis.

Atom	R(a.u.)	$M(\mu_B)$, NRLMOL	$M(\mu_B)$, SIESTA
Fe	2.19	3.85	3.91
O (apical)	1.25	0.20	0.30
O (bridge)	1.25	$\pm$0.01	$\pm$0.02
N	1.32	0.07	0.09

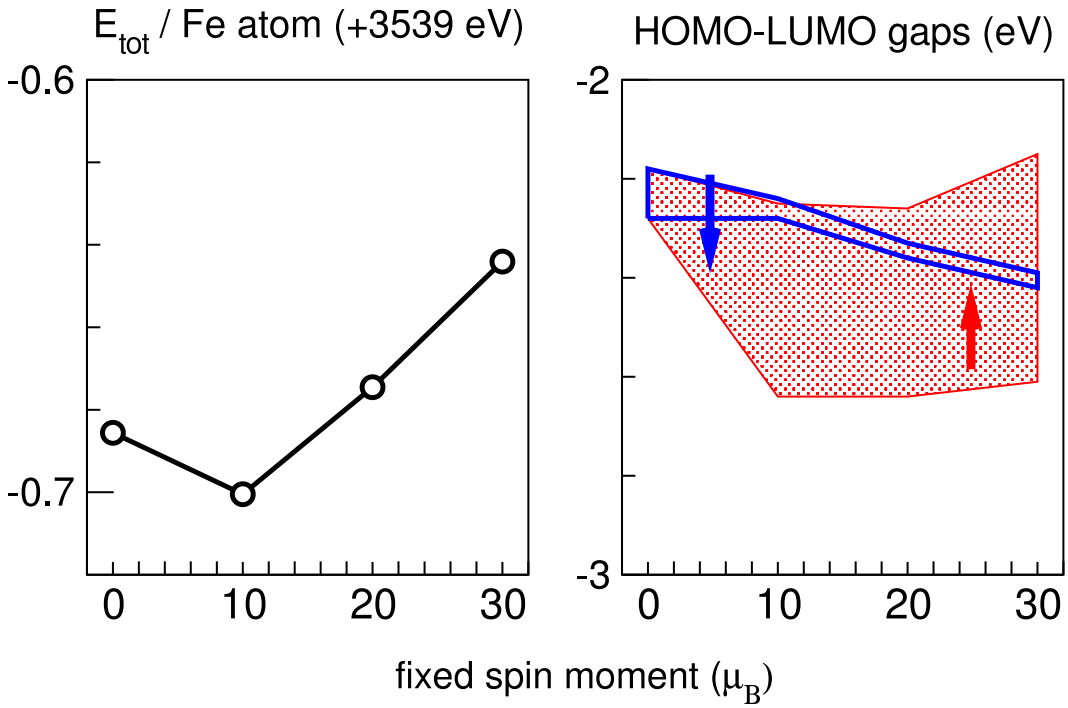

Figure 7: Total energy per Fe atom (left panel) and energy gap in two spin channels (right panel; shaded area – majority-spin, thick lines – minority-spin) from fixed spin moment calculations.

of the total energy while inverting one and then two local moments from the FM configuration is what would be expected from the Heisenberg model with "rigid" magnetic moments (in the sense that their S values do not depend on the total spin of the system), assuming moreover that only nearest-neighbors interactions between spins are important. An additional justification of the validity of the Heisenberg model comes from an observation that the magnitudes of local magnetic moments at Fe atoms always remain close (within several per cent) to 4 $\mu_{\rm B}$, and the partial DOS on Fe sites remains largely unaffected by the actual magnetic ordering. Similarly unaffected is a pattern of local magnetic moments at O and N neighbors of a particular Fe atom, always getting inverted as the latter experiences a spin flip. Keeping this in mind, and assuming Heisenberg-model spin Hamiltonian as in Section 1 with the S value of 5/2 (i.e., for the total spin which gets inverted), we arrive at the estimate for $-J$ of around 80 K (over both 30→20 and 20→10 $\mu_{\rm B}$ flips). This is qualitatively correct (i.e. indicates a preference toward AFM coupling) and even of correct order of magnitude. However, two observations can be made here. First, the "true" AFM configuration (with half of magnetic moments inverted on the ring) does not follow the linear trend (see Fig. 7) and lies actually higher in energy than the configuration with two spins inverted. The origin of this is not yet clear to us at the moment. There are several possibilities, the zero-FSM configuration is, technically,the most difficult to converge, so some numerical instability can still play a role. On the other hand, a true (mixed) quantum-mechanical ground state of a system with six coupled S=5/2 spins may win over both our DFT solutions which correspond to selected values S_z=0 or S_z=5 of the total spin. Moreover, the necessity to include magnetic interactions beyond first neighbors, not yet considered at the moment, might further complicate the situation. The second observation concerns the magnitude of exchange parameter J and the fact that it is probably overestimated by a factor of ∼4 in our calculation.

The origin of this lies most probably in on-site correlations, which, if treated accurately beyond the standard schemes of the DFT, would primarily affect localized Fe3d states, shifting the bulk of occupied states downwards in energy, the bulk of unoccupied states upwards, expanding the energy gap, and – whatever scheme to use for estimating exchange parameters – substantially reducing their magnitude. This has been recently shown for another molecular magnet (Mn_{12}) by Boukhvalov *et al.* (2002) – see the discussion on Mn_{12} above and our analysis of a model binuclear system below.

Summarizing our analysis of the electronic structure of Li- and Na-centered "ferric wheels", one can conclude that *local* magnetic moments on Fe sites seem to be 4 μ_B rather than 5 μ_B as is often assumed. This implies the valence state closer to Fe(II) than to Fe(III), with a substantial covalent part in the Fe–O bonding. The local spin of S=5/2 per iron site consistent with magnetization measurements is however recovered if one takes the magnetization of neighboring atoms into account. The ability to calculate Wannier functions in such systems may provide much more reliable estimates of projected moments than are currently offered by either Mulliken methods or methods based on moments within a sphere. It is the largest on the apical oxygen atom, followed by smaller moments on nitrogen and the bridging oxygen atoms. This picture is well confirmed by a spatial distribution of spin density.

With respect to its magnetic interactions, this system can be mapped reasonably well onto the Heisenberg model; hence we deal with *rigid* magnetic moments which are nevertheless *delocalized* – an interesting counter-example to a common belief that the Heisenberg model primarily applies to localized spins.

5.2 Ni_4

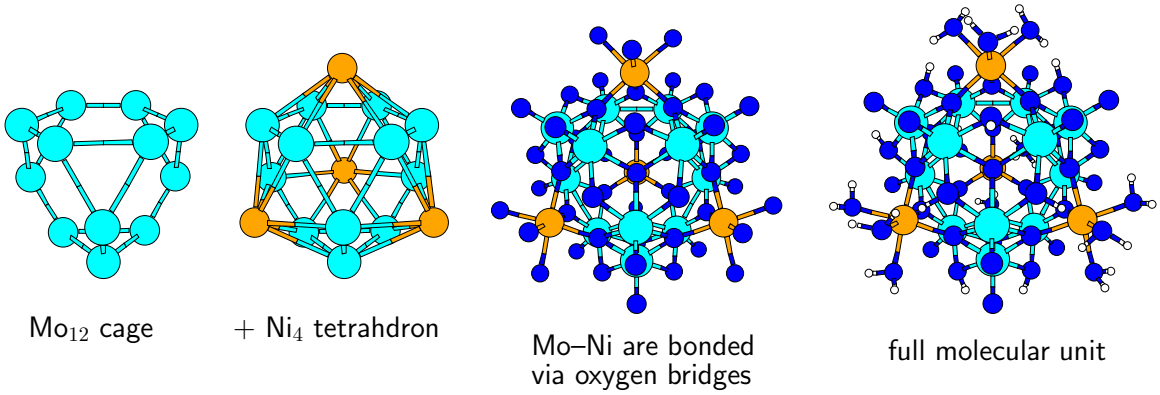

Figure 8: Buildup of the "Ni_4" molecular unit.

"Ni_4" is a shorthand notation for a molecular crystal $[Mo_{12}O_{30}(\mu_2\text{–}OH)_{10}H_2\{Ni(H_2O)_3\}_4] \cdot 14\ H_2O$, synthetisized and characterized by Müller *et al.* (2000). This material crystallizes in a structure containing two formula units (shown in Fig. 8), related by the 180° rotation around an edge of the Ni_4 tetrahedron. The Ni–Ni distance is 6.6–6.7 Å, and magnetic interactions are mediated by a longer path than in the systems discussed above.

Magnetic properties are due to Ni^{II} ions in the $3d^8$ configuration (s=1); the ground state is an-

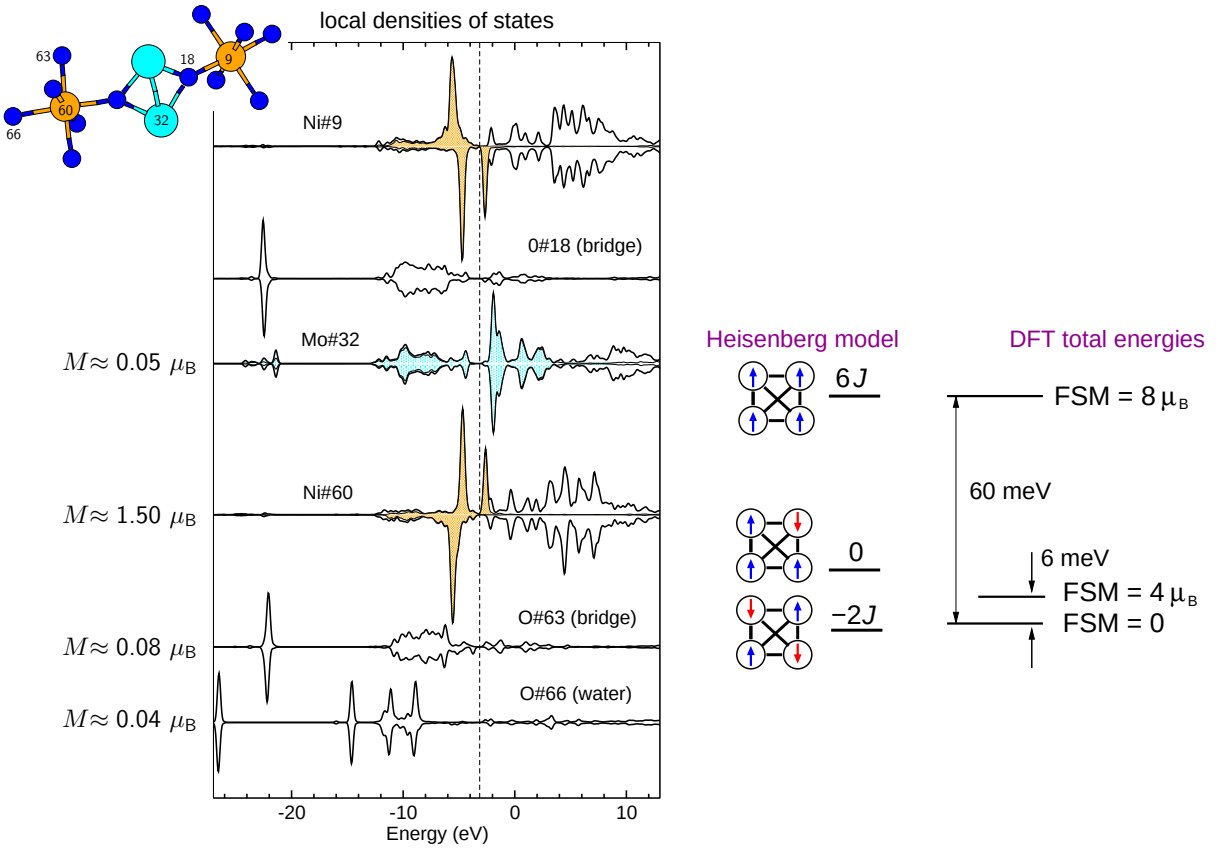

Figure 9: Left panel: local DOS of atoms at the Ni–Ni magnetic path. Right panel: a scheme of energy levels in different spin configurations of "Ni_4" according to the Heisenberg model and from first-principles calculations.

tiferromagnetic. An intriguing aspect of this compound is that the measured zero-field magnetic susceptibility can be very well mapped onto the Heisenberg model, whereas the measurements of magnetization cannot. The inclusion of different anisotropy terms in the Heisenberg model in order to improve the description of experiment had only limited success (Brüger, 2003). First-principles calculations have been performed using the SIESTA method in order to access the electronic structure and estimate the magnitudes of magnetic interaction parameters.

Similarly as in the case of the "ferric-wheel" system discussed above, the FSM scheme was used for pinning down different spin configurations and comparing their total energies. The local DOS is practically indistinguishable for the cases of zero total moment (the AFM structure, which has indeed, in agreement with experiment, the lowest total energy) and configurations with local magnetic moments inverted at one or two Ni atoms (yielding, in the last case, the FM configuration). The local moment per atom in these cases agrees with the s=1 estimation derived from magnetization measurements. As was discussed above for other magnetic molecules, the magnetic moment is not fully localized on the Ni ion; small but non-negligible magnetization is induced on neighboring oxygen atoms, and even on more distant Mo atoms (Fig. 9, left panel). As the Ni–Ni interaction path is much longer than in other earlier discussed magnetic molecules (see inset in Fig. 9), the energy differences between configurations with FSM values

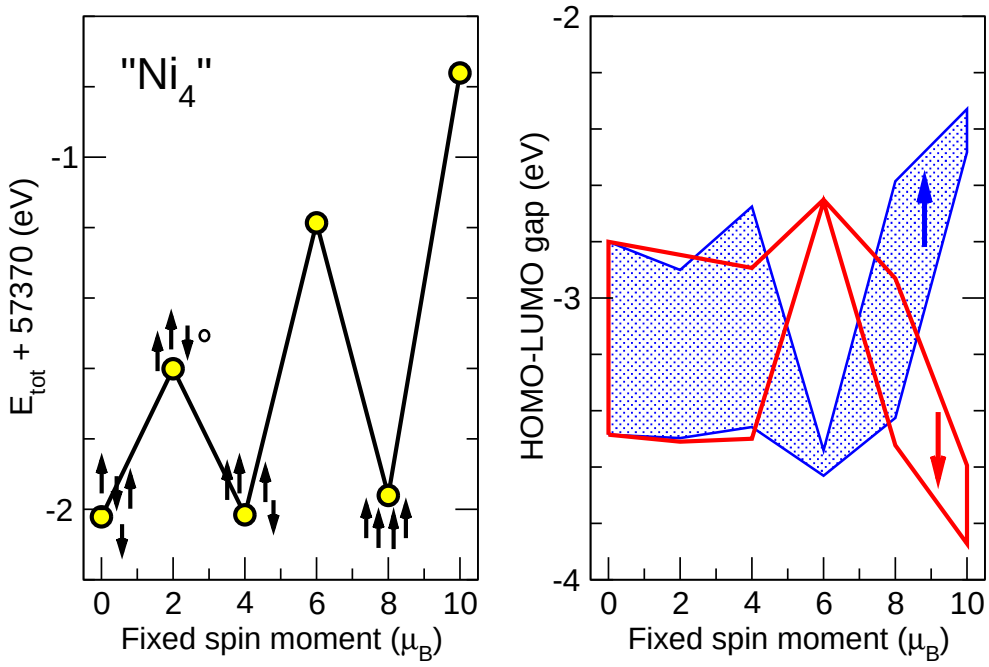

Figure 10: Total energy (left panel) and HOMO-LUMO gap (right panel) from FSM calculations of "Ni_4". See text for details.

of 0, 4 and 8 μ_B are small. These solutions are separated by other magnetic configurations which can be converged (2 and 6 μ_B) and correspond to a non-magnetic configuration of one Ni atom, with unchanged and differently coupled s=1 at three others (as schematically shown in Fig. 10, left panel). Energies of these intermediate configurations are substantially higher, and HOMO-LUMO gaps in two spin channels move apart, indicating the necessity of an external magnetic field (hence additional Zeeman energy) for stabilizing these artificial configurations. On the contrary, the three lowest-energy configurations have HOMO-LUMO gaps common for both spin directions (Fig. 10, right panel), therefore the mapping to the Heisenberg model can be done directly, without considering the Zeeman term.

An attempt of such mapping is schematically shown in the right panel of Fig. 9; obviously the sequence of energies of the configurations with one or two spins inverted (starting from the FM solution) is only in qualitative agreement with the Heisenberg model, but numerical energy differences do not allow for the evaluation of a unique value of J, in contrast to the case of "ferric wheel" discussed above. At best, one can make a rough estimate of the order of magnitude of $-J$, that yields 30 – 90 K.

This failure suggests that the magnetic interactions in "Ni_4" are strongly anisotropic. However, an adequate mapping of first-principles results onto models including the anisotropy would require the inclusion of spin-orbit interaction in the calculation, and this is not yet available in SIESTA. This feature is however included in NRLMOL and some of the progress along these lines is outlined below.

5.3 Magnetic anisotropy in single molecule magnets

As a modification of Eq. (4) which introduced the anisotropy in the simplest form, we distinguish in the following between axial and transverse anisotropy, with their corresponding parameters D and E. They enter the magnetic spin Hamiltonian (only second order terms) as follows:

$$\mathcal{H} = DS_z^2 + E(S_x^2 - S_y^2), \tag{43}$$

The values of the axial anisotropy D are available from a number of experiments for different SMM, and for several SMM first-principle calculations have been carried out with the use of the NRLMOL code. These results are summarized in Table 3.

Table 3: Comparison of the calculated by NRLMOL and experimental magnetic anisotropy parameter D for the single molecule magnets. See theory references for computational details.

Molecule	S	D(K)	
		Theory	Experiment
$Mn_{12}O_{12}(O_2CH)_{16}(H_2O)_4$	10	-0.56^a	-0.56^b
$[Fe_8O_2(OH)_{12}(C_6H_{15}N_3)_6Br_6]^{2+}$	10	-0.53^c	-0.30^d
$[Mn_{10}O_4$(2,2'-biphenoxide)$_4Br_{12}]^{4-}$	13	-0.06^e	-0.05^f
$Co_4(CH_2C_5H_4N)_4(CH_3OH)_4Acl_4$	6	-0.64^g	-0.7 – -0.9^h
$Fe_4(OCH_2)_6(C_4H_9ON)_6$	5	-0.56^i	-0.57^j
$Cr[N(Si(CH_3)_3)_2]_3$	3/2	-2.49^i	-2.66^k
$Mn_9O_{34}C_{32}N_3H_{35}$	17/2	-0.33	-0.32^l
$Ni_4O_{16}C_{16}H_{40}$	4	-0.385	-0.40^l
$Mn_4O_3Cl_4(O_2CCH_2CH_3)_3(NC_5H_5)_3$	9/2	-0.58^m	-0.72^n

[a]Pederson and Khanna (1999a,b), [b]Barra *et al.* (1997); Mertes *et al.* (2001), [c]Kortus *et al.* (2001b), [d]Dressel *et al.* (2003), [e]Kortus *et al.* (2002a), [f]Barra *et al.* (1999), [g]Baruah and Pederson (2002), [h]Murrie *et al.* (2003), [i]Kortus *et al.* (2002c), [j]Schromm *et al.* (2003), [k]Bradley *et al.* (1973), [l]Rajaraman and Wimpenny, [m]Park *et al.* (2003c), [n]Wernsdorfer *et al.* (2002).

In all the cases presented here the calculated spin ordering is in agreement with experiment. The calculated D parameters for Mn_{12}, Mn_{10}, Mn_9, the ferric star Fe_4 and Cr-amide molecular magnets are in excellent agreement with experimental values. The only remarkable discrepancy is found for Fe_8, a system which seems to pose complications for the DFT treatment. Apparently the DFT may be unable to predict the ground state density accurately enough due to important electronic correlations beyond the mean-field treatment or missing Madelung stabilization (absent in the isolated system).

The SMM listed in Table 3 are in general characterized by a high spin ground-state. However, a high spin state does not necessarily correlate with a high anisotropy barrier. The prefactor D is also very important. In order to increase the barrier one has to understand and control D, which will be the main goal of future research in this area. In all cases where the E parameter is

not zero by symmetry it has been predicted with similar accuracy as D – see relevant references for details.

The results obtained make one confident in the predictive power of the formalism. It has been already mentioned that a microscopic understanding (based on the electronic structure of SMM) of the magnetic anisotropy parameters is crucial for the rational design of single molecule magnets.

In the following we will discuss some selected recent results of the not so well known single molecule magnets.

5.3.1 Co_4 magnet

A new Co-based ferromagnetic SMM with the complete chemical formula $Co_4(hmp)_4(CH_3OH)_4Cl_4$ (hmp^- is the deprotonated hydroxymethylpyridine), has achieved great interest due to the high anisotropy energy. A simulation by Baruah and Pederson (2002) resulted in the prediction of two new, energetically noncompetitive structural conformations with even higher anisotropy. Specifically, the magnetic anisotropy energy per Co atom was estimated from the experiment to be 25–50 K (Yang *et al.*, 2002). Although, newer experiments on a similar Co_4-cluster find significantly smaller total anisotropy energies of about 29 K (Murrie *et al.*, 2003), in better agreement with calculated values of 23, 160 and 50 K for the lowest energy and two higher energy phases found in the calculation. As already mentioned above, a large magnetic anisotropy is a prerequisite for potential applications of molecular magnets as "microdomains" for magnetic storage. An additional requirement, the existence of a net spin moment, is also satisfied here, with S=6 per molecular unit in the parallel (high spin) configuration, in all three isomers. Especially given that the earlier calculated results of Baruah *e*t al. compare more favorably with the more recent experimental results, a first-principle calculation might guide and stimulate practically relevant experimental research on this promising family of molecular magnets.

5.3.2 Fe_4-star

This material (of which several analogues with different central atom are known by now) realizes net spin moment in relatively compact and highly symmetric molecule due to AFM coupling of peripheric Fe atoms to the central one. The structure of the Fe_4 "ferric star" is shown in Fig. 11. All iron atoms are in the Fe^{3+} state, and the resulting ferrimagnetic arrangement has total $S = 5$. Similar to the other molecular magnets only states within an energy window of about 5 eV around the Fermi level contribute to the magnetic anisotropy. The symmetry of the cluster allows for a rhombohedral E contribution to the spin Hamiltonian. Using the experimental geometry (Schromm *et al.*, 2003) as a starting point for the calculation the theoretical value of $|E|$=0.064 K is in good agreement with the experimental one ($|E|$=0.056 K). [12] This agreement is relatively stable with respect to geometry changes. Total anisotropy barriers change normally only by a few K at most, although in some cases the agreement between theory and experiment becomes worse by optimizing the molecular geometry in the calculations. This can be understood because the geometry optimization is done for a single isolated molecule neglecting crystal packing effects

[12] The sign of E depends on the definition of the axis.

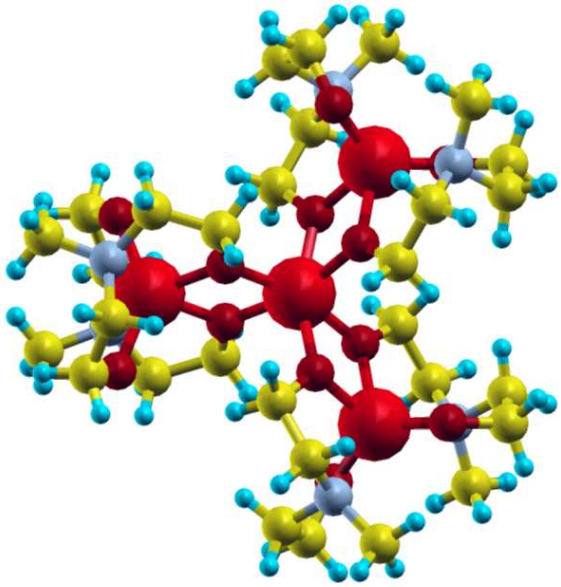

Figure 11: The molecular structure of the Fe_4-star. The Fe atoms are shown by large spheres.

and interactions in the molecular crystal which are important for the real molecular geometry.

5.3.3 Mn_{10} cluster

Ten Mn atoms form a tetrahedron-like structure with Mn atoms at the corners and at the middle of the tetrahedron edges, all bridged by oxygen ions (Barra *et al.*, 1999). Two of the Mn atoms are coupled antiferromagnetically to all the rest. The calculation by Kortus *et al.* (2002a) suggests an ionic picture that the first Mn has an Mn^{3+} ($S = 2$) state, whereas the other two are Mn^{2+} ($S = 5/2$). Due to the symmetry of the cluster, the two types of majority spin Mn atoms have a multiplicity of 4 whereas the minority spin Mn atom has a multiplicity of 2, resulting in the $S = 4\times2+4\times5/2-2\times5/2 = 13$ magnetic ground state. This magnetic core is further stabilized by organic rings which are also connected to the oxygen atoms. This molecular unit with the chemical formula $[Mn_{10}O_4(2,2'\text{-biphenoxide})_4Br_{12}]^{4-}$ is charged and compensated by another molecular cluster containing a single manganese atom, $[(CH_3CH_2)_3NH]_2[Mn(CH_3CN)_4(H_2O)_2]$.

The calculations confirms the experimental suggestion that the magnetic anisotropy is only due to the functional unit containing 10 Mn atoms. The compensating cluster behaves paramagnetically with the Mn atom in a +2 charge state and spin $s = 5/2$. As shown by Kortus *et al.* (2002a), the single Mn-complex exhibits the easy-plane behavior with the energy well of only 0.1 K. The majority-spin gap in Mn_{10} is much smaller than the minority-spin one. Those matrix elements of Eq. (35) related to the occupied majority-spin states contribute in favor of an easy axis behavior whereas the matrix elements from the occupied minority-spin channel favor easy plane. These tendencies compete and cancel each other to a large extent. Only due to the larger contribution from the occupied majority-spin channel the complete Mn_{10} cluster ends up as an easy-axis system. Therefore, in spite of the fact that Mn_{10} possesses a high-spin state (S is larger than in Mn_{12}-ac), the anisotropy barrier in this system is small. Kortus *et al.* (2002a)

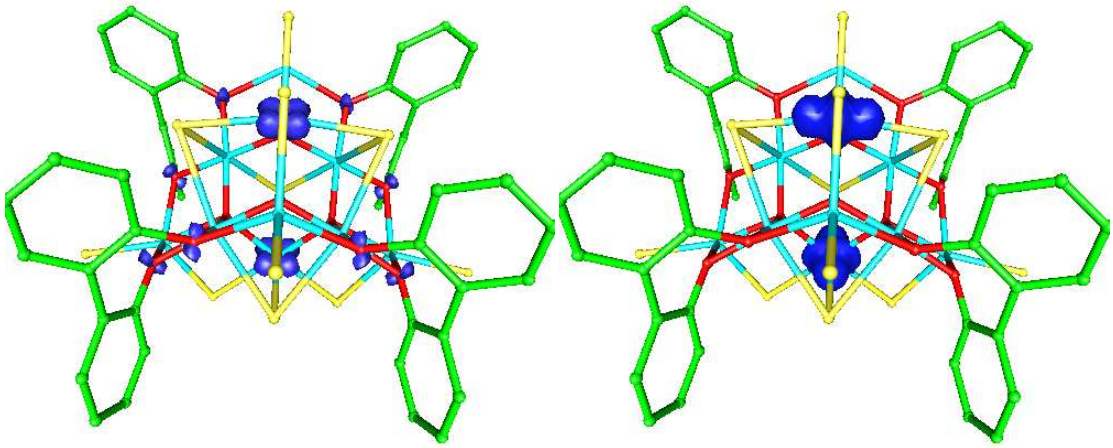

a) b)

Figure 12: Isosurface (dark blue) at 0.005 e/a_B^3 of the square of the wavefunctions (a: occupied majority state; b: unoccupied minority state) that contribute most to the matrix elements $M_{ij}^{\sigma\sigma'}$ of Eq. (35). Light blue: Mn, yellow: Br, red: O, green: C atoms. It is clearly visible that the matrix element connects majority and minority d-states at the same Mn atom.

found that the removal of subsets of the Br ions will change the magnetic anisotropy drastically due to large perturbations of the electronic structure. However, neutralizing the electric field due to Br ions by an external potential in the calculations changed the anisotropy barrier by less than 1 K. Therefore, one can conclude that the electric fields created by the Br ions do not have any significant effect on the magnetic properties of the molecule, in contrast to chemical interactions.

One of the advantages of the first-principles approach is the possibility to control in detail the interactions and states which are important for a certain physical property in order to gain a microscopic understanding. Eq. (35) shows that the barrier is related to matrix elements between occupied and unoccupied orbitals in the majority and minority spin channels. Besides the discrimination associated with spin pairing, we can analyze which electronic states mostly contribute to the matrix elements $M_{ij}^{\sigma\sigma'}$. In Fig. 12 we display plots of the square of the wavefunctions of the occupied majority state and the unoccupied minority state that contribute to the matrix element $M_{ij}^{\sigma\sigma'}$ with the largest absolute value.[13] It is clearly visible that the states of interest are d-states localized at the same Mn atom. In this case, the states are localized at the minority spin Mn atoms.

5.4 Some results of the V_{15} spin system

As already mentioned, the V_{15} system remains of great interest for studies on quantum coherence and relaxation phenomena, despite not having any sizeable magnetic anisotropy barrier (Chaboussant *et al.*, 2002; Chiorescu *et al.*, 2000; Gatteschi *et al.*, 1991; Kortus *et al.*, 2001a). The dynamics of the magnetization relaxation depends on the spin-phonon interaction at finite temperatures and an intrinsic phonon-bottleneck with a characteristic 'butterfly' hysteresis has

[13] Please note, that the value of the magnetic anisotropy energy is not determined by a single dominant contribution, but results from the sum of many contributions with different signs.

been demonstrated by Chiorescu *et al.* (2000). Due to several very recent experimental studies on this system it became possible to check the quality of the electronic structure calculation. In a joint theoretical and experimental study by Boukhvalov *et al.* (2003) the system has been investigated using the LSDA+U band structure calculations [the same computational method as referred to above, for calculations by the same group on Mn_{12}-ac, Boukhvalov *et al.* (2002)] and measured X-ray photoelectron and fluorescence spectra. Comparing experimental data with the results of electronic structure calculations the authors conclude that the LMTO LSDA+U method provides a good description of the electronic structure of V_{15}.

Choi *et al.* (2003) report the reflectance and optical conductivity of solid V_{15} over a wide energy range. The band centered at 1.2 eV is assigned as a V dd transition, and other features at 3.7, 4.3, and 5.6 eV are attributed to Op-Vd charge transfer excitations. The comparison of the results to recent electronic structure calculations (Boukhvalov *et al.*, 2003; Kortus *et al.*, 2001a,b) show good agreement with all these calculations without clearly favoring any U value.

Chaboussant *et al.* (2002) report an Inelastic Neutron Scattering study of the fully deuterated molecular compound. They deliver direct confirmation that the essential physics at low temperature is determined by three weakly coupled spin-(1/2) on a triangle. Interestingly, the experiment allowed to determine the effective exchange coupling of 0.211 meV within the triangle and the gap between the two spin-(1/2) doublets of the ground state. This direct interaction had been predicted earlier by Kortus *et al.* (2001a) with an value of 0.55 meV.

The work by Kortus *et al.* (2001a) utilized an efficient coupled multilevel analysis which relied on fitting density-functional energies to mean-field Heisenberg or Ising energies in order to determine the exchange parameters. The approximate exchange parameters gleaned from the first N Ising configurations were used to find the next lowest energy Ising configuration and subsequently to improve the parameterization of the exchange parameters. The "self consistency" criterion in this approach was the check as to whether the predicted Ising levels remain unchanged under the addition of data from new Ising configurations. This mapping of DFT results on a classical Ising model allowed for the determination of the exchange parameters by considering only several spin configurations.

The data used to determine the exchange parameters from a least square fit to the mean-field solution of the Heisenberg Hamiltonian (Eq. 2) are displayed in Table 4. The fit is very good (with errors ranging from 0.1 to 1.55 meV) and leads to exchange parameters (in the notations of Fig. 4) of $J = 290.3$ meV, $J' = -22.7$ meV, J''=15.9 meV, $J1 = 13.8$ meV, $J2 = 23.4$ meV and $J3 = 0.55$ meV, where positive numbers correspond to AFM and negative to FM interactions. The *ferromagnetic* interaction J' is a surprising result and deserves further discussion since it is qualitatively different from earlier assumptions based on entirely AFM interactions (Chiorescu *et al.*, 2000; Gatteschi *et al.*, 1991). A FM coupling is possible without polarizing the oxygens through a fourth order process similar to super-exchange. In super-exchange, the intermediate state has the lowest d-orbital on the V atom doubly occupied with up and down electrons. However, electrons can also hop to higher energy d-orbitals. In this case both parallel and antiparallel spins are allowed without violating the Pauli exclusion principle, and consistently with the Hund's first rule the parallel spin alignment is preferred. The superexchange (within the same d-orbital) completely excludes the electrons of the same spin electrons whereas the

Table 4: DFT energies (E in meV) of calculated Ising configurations, energies obtained from the fit, and $4\langle S_i^q S_j^q \rangle$ along each of the six bonds. Also included is the anisotropy shift δ for the $M_s = S$ state of each Ising configuration. A least square fit of this data leads to exchange parameters of J=290.3, J'=−22.7, J"=15.9, $J1$=13.8, $J2$=23.4 and $J3$=0.55 meV.

E	Fit	J	J'	J''	$J1$	$J2$	$J3$	Spin	Label	δ (K)
−78.37	−78.44	−6	2	−2	6	−6	−1	1/2	I	0.8
−73.39	−73.63	−6	2	−2	4	−4	−1	1/2	II	
−35.48	−35.08	−6	−2	2	4	−4	−1	1/2	III	
−34.89	−34.53	−6	−2	2	4	−4	3	3/2	IV	
0.00	−0.79	−6	−6	6	6	−6	3	3/2	V	1.5
8.38	8.28	−6	−6	6	2	−2	−1	1/2	VI	1.3
28.14	28.08	−6	−6	6	−6	6	3	3/2	VII	
126.32	126.14	−4	−4	6	4	−6	3	1/2	VIII	
129.17	128.88	−4	−4	2	6	−4	3	5/2	IX	
278.35	278.50	−2	−6	2	4	−4	3	3/2	X	
434.22	435.78	0	0	6	6	0	3	9/2	XI	1.6
760.75	760.76	6	6	6	−6	−6	3	9/2	XII	1.6
873.11	872.35	6	6	6	6	6	3	15/2	XIII	1.8

ferromagnetic process (different participating d-orbitals) merely favors FM alignment. Thus a FM coupling is obtained if the V-O hopping matrix elements into the higher d-orbital are significantly larger than the matrix elements for the hopping of O electrons into the lowest energy d-orbital. The occurrence of such interactions are possible in a low-symmetry system such as V_{15}. Even with this FM interaction, the spin Hamiltonian yields an S=1/2 ground state composed largely of Ising configurations similar to the one depicted in Fig. 4. This Ising configuration was predicted from the J's from the earlier fits to DFT energies and corresponds to the ground state DFT configuration (I).

Comparing the calculated susceptibility with experiment (Chiorescu *et al.*, 2000), one finds the that low-temperature behavior is not well reproduced and the doublet-quadruplet gap $\Delta \approx 10$K is significantly larger than the experimental value of $\Delta \approx 3.7$K, while the high-temperature behavior shows that calculated value of J is too large.

Both of these discrepancies can be explained almost entirely by a J that is too large within the density-functional-based treatment. The large value of J can be attributed to both exchange processes through the oxygens and to direct exchange between the V. If direct exchange is important, the value of J will be influenced greatly by the overlap between the V atoms. Electronic correlations included in form of LDA+U may help to improve the agreement with experiment, because the overlap between the d-orbitals of the vanadium atoms will be decreased by shifting the occupied d-orbitals down in energy by U. Similarly, self-interaction corrections (SIC) (Svane and Gunnarsson, 1988, 1990) will lower the magnitude of J because it will localize the V d-orbitals more, reducing the overlap of the wavefunctions.

Without including a direct exchange interaction between the vanadium atoms in the inner triangle ($J3 = 0$), reducing J to 70 meV and slightly reducing the difference between $J1$ and $J2$ yields the experimentally observed effective moment. Although, another set of only antiferromagnetic interactions (Gatteschi *et al.*, 1991) also fits the experimental results well. In fact any set of parameters with the correct values of J and Δ given by simple perturbation theory

$$\Delta = \frac{3}{4}\frac{(J2 - J1)^2(J'' - J')}{J^2} + \frac{3}{2}J3, \tag{44}$$

will fit the experimental effective moment well. The already mentioned problem of the parameter dependence on the assumed model arises here.

By including a possible direct interaction between the triangle vanadium atoms ($J3$) in the spin Hamiltonian the agreement with experiment can be achieved by dividing all J's by a constant factor of 2.9. Scaling of $J3$ down by a factor of 2.9 gives a value of 0.19 meV, in surprisingly good agreement with the corresponding value obtained from inelastic neutron scattering (Chaboussant *et al.*, 2002) of 0.221 meV. One possibility to decide between different models could be the measurement of the spin ordering and the spin-spin correlation functions by, e.g., neutron scattering.

5.5 A model Fe-binuclear system

Binuclear metal-organic systems form a large, and probably simplest, group among molecular magnets. Even if their magnetic characteristics like ordering temperature and bulk magnetization are not necessarily outstanding, they help to grasp important physics of $3d$–$3d$ magnetic interaction mediated by an organic ligand and thus offer a convenient model system. Moreover, an interesting effect of spin-crossover has been observed in some such systems, for instance in $[Fe(bt)(NCS)_2]_2$-bpym (bt= 2,2'-bithiazoline, bpym= 2,2'-bipyrimidine): a switch from LS-LS to LS-HS to HS-HS configuration (LS: low spin; HS: high spin) at the increase of temperature, where the intermediate LS-HS state gets stabilized near 170 K due to an interplay between intermolecular and intramolecular magnetic interactions (Ksenofontov *et al.*, 2001a,b; Létard *et al.*, 1999). One demonstrated the possibility of optical switching between different magnetic states and brought into discussion the prospects of their use as active elements in memory devices.

Our interest in binuclear systems is primarily that for model molecular magnets, to be treated with a method of recognized accuracy, and with the aim to look at the effect of intraatomic correlation effects ("Hubbard U"). Starting from the real structure of $[Fe(bt)(NCS)_2]_2$-bpym (see Fig. 13, left panel), we "streamlined" it somehow to fit it into a compact unit cell for an accurate calculation by a band structure method with periodic boundary conditions (Fig. 13, right panel). This transformation preserved the bipyrimidine part between two Fe centers, but "shortcut" the distant parts of ligands to make a connected structure. The calculation has been done with the FLEUR code (FLEUR homepage), a realization of full-potential augmented plane wave technique. One can see that, in contrast to "ferric wheels", the Fe atom is now octahedrally coordinated by nitrogen ions. A formal valence state in these compounds is routinely referred to as Fe(II). The HS and LS states were discussed to be represented by the $t_{2g}^4 e_g^2$ and t_{2g}^6 configurations, correspondingly (Ksenofontov *et al.*, 2001b). Our calculation did not yet include

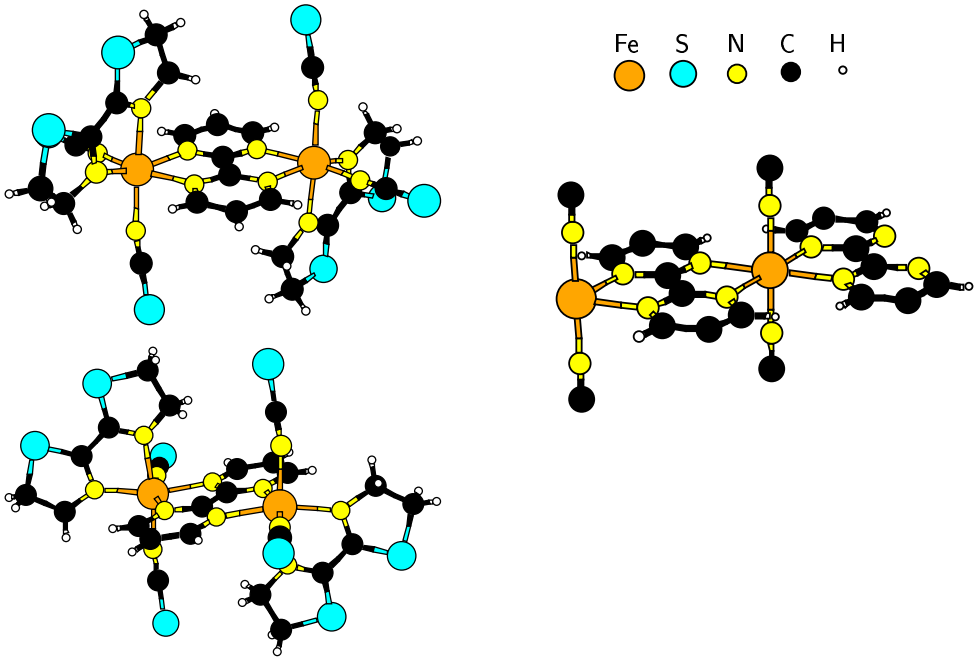

Figure 13: Two views of the $[Fe(bt)(NCS)_2]_2$-bpym molecule (left panel) and a simplified periodic Fe-binuclear system used in the FLEUR calculation (right panel).

the orbital transition of this type; we initialized only HS configurations and brought them into self-consistency in FM and AFM settings. The resulting partial DOS are shown in Fig. 14.

Certain similarities can be found with the Fe local DOS in "ferric wheels" – clear splitting into t_{2g}-like and e_g-like states in nearly octahedral ligand field, full occupation of majority-spin Fe3d states and one electron per Fe atom trapped in the Fe3d–N2p hybridized band of minority spin. The values of magnetic moments (total per Fe atom in the FM case, along with the local moment, integrated over the muffin-tin sphere) are listed in Table 5. The interatomic exchange parameters have been estimated from total energy differences between FM and AFM cases.

Table 5: Magnetic moments and interaction parameters as estimated for a model Fe-binuclear system (Fig. 13) from calculations by FLEUR with and without Hubbard U.

		M(Fe)	M/Fe	ΔE	J (S=5/2)
$U=0$	FM	3.62	4.10		
	AFM	3.61	–	102.5 meV	−190 K
$U=4$ eV	FM	3.93	4.94		
	AFM	3.92	–	76.8 meV	−143 K

Since the magnetic moment is largely localized at the Fe site, the inclusion of intraatomic correlations beyond the "conventional" DFT might be important. The exchange parameters J depend on the spatial overlap of the d-orbitals on different Fe-sites. It is well known that the d-orbitals within DFT are not localized enough compared to experiment, consequently the J values will be overestimated. There are two main reasons for this shortcoming. First, possible on-site

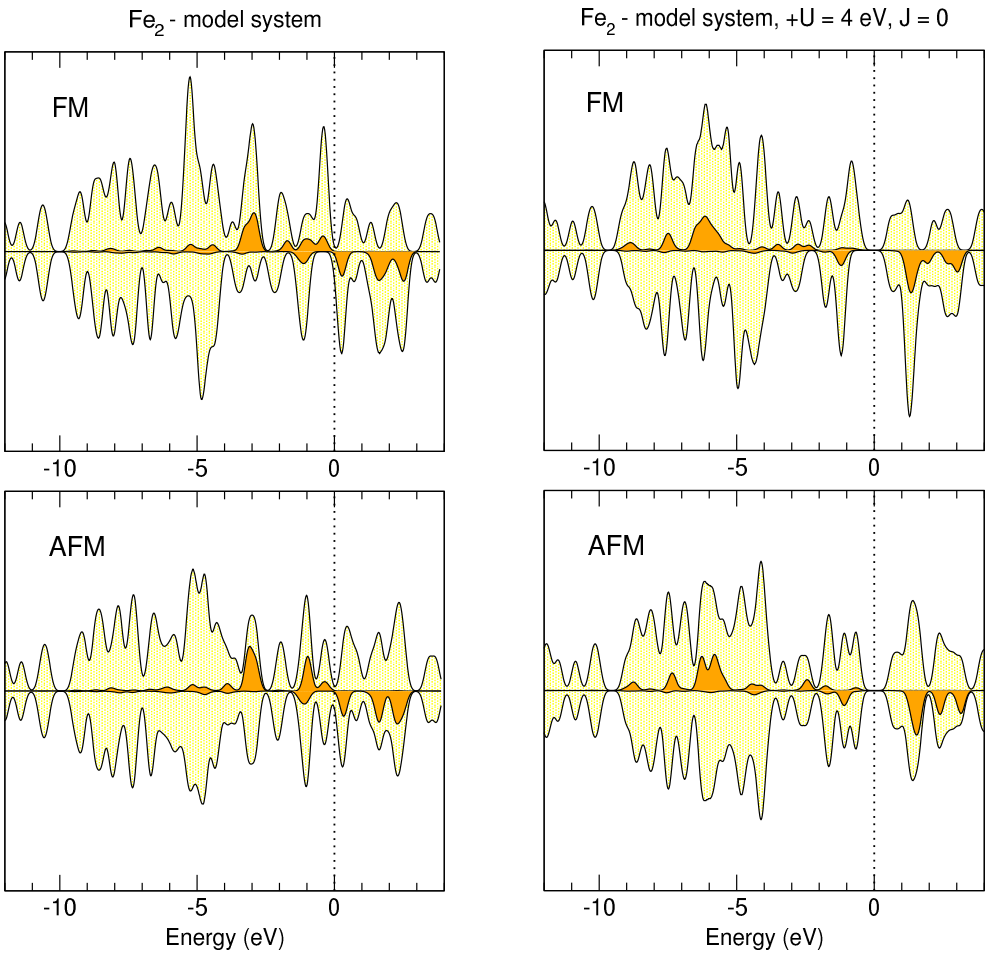

Figure 14: Densities of states in FM and AFM cases as calculated by FLEUR for the model Fe-binuclear system, in the DFT and in the LDA+U approach. Fe local DOS are shown as shaded areas.

correlations as known from atomic physics are underestimated in case of "conventional" DFT. Second, DFT is not free from spurious self-interactions due to the replacement of the point-like electrons by corresponding densities. Bringing in the atomic physics in the form of LDA+U (adding a local orbital dependent atomic Coulomb interaction parameter U to DFT (Anisimov *et al.*, 1997) or self-interaction corrections (SIC) (Svane and Gunnarsson, 1988, 1990) will improve the results by lowering the d-orbitals in energy and therefore localizing them stronger. SIC only affects occupied states, whereas LDA+U plunges the occupied d-states and shifts the unoccupied ones to higher energies. By increasing, on the average, the magnetic excitation energy across the spin majority-minority gap, both mechanisms help to effectively reduce the magnitude of J. To our knowledge, SIC have not yet been applied in calculations on molecular magnets (nor, are we aware of any practical implementation of SIC in a full-potential code, i.e., beyond the muffin-tin- or atomic sphere approximation. Baruah *et al.* are actively working toward a practical implementation of SIC within the NRLMOL suite of codes. The LDA+U scheme is implemented in the FLEUR code (as in many others). This *ansatz* has however a disadvantage of not being truly first-principles one: it remains on the user to single out certain orbitals as localized and to choose an appropriate value for the "Hubbard U" parameter. For

Fe-binuclear system we have chosen an empirically reasonable value U=4 eV; in principle, we were more interested in studying qualitative trends, as it deals with a model system anyway. One observes from Table 5 that the inclusion of intraatomic correlation enhances somehow the local magnetic moment at th Fe site, and to a much smaller extent – the total magnetic moment (in the FM configuration). Much more important, the J parameter is noticeably reduced due to correlation included. These observations agree with what was earlier reported by Boukhvalov *et al.* (2002) for the "Mn_{12}" system from the LDA+U calculation.

6 Conclusion

We attempted to give a broad overview of physical questions and technical problems one faces in modern first-principles simulations in the rapidly growing field of molecular magnets. Our own presented results largely correspond to work still in progress, and they might be far from providing an ultimative answer for particular systems. On the contrary, the results are likely to be refined and extended by subsequent studies. Our current results make us very confident in the predictive power of the presented methods. In order to explore the range of systems where the presented first-principles methods give reliable results, further studies on more systems are required. A large number of calculations are being performed by other groups on many other systems, which we might fail to name in this limited contribution. However, it is our hope that it may help the newcomers in the field to access the problems, the difficulties experienced and the possibilities offered by different methods and practical schemes of first-principles calculation. Many additional calculations are required to obtain a complete understanding of the idealized behaviors of molecular magnets and both new theory and new computational tools will be required to understand the nonidealities which will define the operating environments in applications of such systems.

Acknowledgments

The authors thank the Deutsche Forschungsgemeinschaft for financial support (Priority Program SPP 1137 "Molecular Magnetism") and appreciate useful discussions with Jürgen Schnack, Stefan Blügel, Sorin Chiuzbăian, Manfred Neumann, Danila Boukhvalov, Vladimir Mazurenko, Vladimir Anisimov and Mikhail Katsnelson. We are grateful to Lilia Boeri, Kyungwa Park and José Soler for critically reading the manuscript. We followed enlightening lectures by Prof. Heiko Lueken at the SPP 1137 Workshop in Magnetochemistry (Kaiserslautern, 2003) in presenting some textbook information in Sec. 3.2 and 3.3. The crystal structure data for calculations of some molecular magnets have been kindly provided by the group of Rolf Saalfrank of the University Erlangen-Nürnberg, Roberta Sessoli of the University of Florence and Paul Kögerler of the Ames Laboratory. A.V.P. thanks Gustav Bihlmayer for introduction into the FLEUR code and for his help in performing the calculations on a Fe-binuclear system. M.R.P. was supported in part by the Office of Naval Research. A.V.P. was supported in part by the Research Council of the President of the Russian Federation (Grant NSH-1026.2003.2) and Russian Foundation for Basic Research (Project 02-02-16674).

References

Abbati, G. L., A. Cornia, A. C. Fabretti, A. Caneschi *et al.* (1998). A ferromagnetic ring of six manganese(III) ions with a S=12 ground state. *Inorg. Chem.* **37**, 1430.

Abbati, G. L., A. Cornia, A. C. Fabretti, W. Malavasi *et al.* (1997). Modulated magnetic coupling in alkoxoiron(III) rings by host-guest interactions with alkali metal cations. *Inorg. Chem.* **36**, 6443.

Andersen, O. K. and O. Jepsen (1984). Explicit, first-principles tight-binding theory. *Phys. Rev. Lett.* **53**(27), 2571.

Andersen, O. K., O. Jepsen and M. Sob (1987). *Linearized band structure methods*, volume 283 of *Lecture Notes in Physics*, 1–57. Springer-Verlag, Berlin–Heidelberg–New York.

Anisimov, V. I., F. Aryasetiawan and A. I. Lichtenstein (1997). First-principles calculations of the electronic structure and spectra of strongly correlated systems: the LDA+U method. *J. Phys.: Condens. Matter* **9**(4), 767.

Antropov, V. P., M. I. Katsnelson and A. I. Liechtenstein (1997). Exchange interaction in magnets. *Physica B* **237–238**, 336.

Banister, A. J., N. Bricklebank, I. Lavender, J. M. Rawson *et al.* (1996). Spontaneous magnetization in a sulfur-nitrogen radical at 36 K. *Angew. Chemie – Intern. Edition in English* **35**(21), 2533.

Barbara, B. and L. Gunther (1999). Magnets, molecules and quantum mechanics. *Physics World* **12** (3), 35.

Barra, A. L., A. Caneschi, D. Gatteschi, D. P. Goldberg *et al.* (1999). Slow magnetic relaxation of $[Mn_{10}O_4(biphen)_4Br_{12}]$ (biphen=2,2'-biphenoxide) at very low temperature. *J. Solid State Chemistry* **145**, 484.

Barra, A. L., D. Gatteschi and R. Sessoli (1997). High-frequency EPR spectra of a molecular nanomagnet: Understanding quantum tunneling of the magnetization. *Phys. Rev. B* **56**, 8192.

Baruah, T. and M. R. Pederson (2002). Electronic structure and magnetic anisotropy of the $[Co_4(hmp)_4(CH_3OH)_4Cl_4]$ molecule. *Chem. Phys. Lett.* **360**, 144.

Baruah, T. and M. R. Pederson (2003). Density functional study of the conformers of Co_4-based single-molecule magnet. *Int. J. Quant. Chem.* **93**, 324.

Bobadova-Parvanova, P., K. A. Jackson, S. Srinivas and M. Horoi (2002). Density-functional investigations of the spin ordering in Fe_{13} clusters. *Phys. Rev. B* **66**, 195402.

Boukhvalov, D. W., E. Z. Kurmaev, A. Moewes, D. A. Zatsepin *et al.* (2003). Electronic structure of magnetic molecules V_{15}: LSDA+U calculations, x-ray emissions, and photoelectron spectra. *Phys. Rev. B* **67**(13), 134408.

Boukhvalov, D. W., A. I. Lichtenstein, V. V. Dobrovitski, M. I. Katsnelson *et al.* (2002). Effect of local Coulomb interactions on the electronic structure and exchange interactions in Mn_{12} magnetic molecules. *Phys. Rev. B* **65**(18), 184435.

Bradley, D. C., R. G. Copperthwaite, S. A. Cotton, K. D. Sales *et al.* (1973). 3-coordinated transition-metal compounds. 3. electron-spin resonance studies on tris(bistrimethylsilylamido) derivatives of titanium, chromium, and iron. *J. Chem. Soc., Dalton Trans.* **1**, 191.

Brechin, E. K., O. Cador, A. Caneschi, C. Cadiou *et al.* (2002). Synthetic and magnetic studies of a dodecanuclear cobalt wheel. *Chem. Commun.* **17**, 1860.

Briley, A., M. R. Pederson, K. A. Jackson, D. C. Patton *et al.* (1998). Vibrational frequencies and intensities of small molecules: All-electron, pseudopotential, and mixed-potential methodologies. *Phys. Rev. B* **58**, 1786.

Brüger, M. (2003). Einfluss der Anisotropie auf die Eigenschaften magnetischer Moleküule am Beispiel des Ni_4-Moleküls. *Diplomarbeit, Universität Osnabrück.*

Caciuffo, R., G. Amoretti, A. Murani, R. Sessoli *et al.* (1998). Neutron spectroscopy for the magnetic anisotropy of molecular clusters. *Phys. Rev. Lett.* **81**, 4744.

Caneschi, A., A. Cornia, A. Fabretti, S. Foner *et al.* (1996). Synthesis, crystal structure, magnetism, and magnetic anisotropy of cyclic clusters comprising six iron(III) ions and entrapping alkaline ions. *Chem.-Eur. J.* **2**, 1379.

Caneschi, A., A. Cornia, A. C. Fabretti and D. Gatteschi (1999). Structure and magnetic properties of a dodecanuclear twisted-ring iron(III) cluster. *Angew. Chem. Int. Ed. Engl.* **38**, 1295.

Caneschi, A., A. Cornia and S. J. Lippard (1995). A cyclic hexairon(III) complex with an octahedrally coordinated sodium-atom at the center, an example of the [12]Metallacrown-6 Structure Type. *Angew. Chemie Int. Ed. Engl.* **34**, 467.

Caneschi, A., D. Gatteschi, R. Sessoli, A. L. Barra *et al.* (1991). Alternating current susceptibility, high field magnetization, and millimeter band EPR evidence for a ground S=10 state in $[Mn_{12}O_{12}(CH_3COO)_{16}(H_2O)_4]\cdot 2CH_3COOH\cdot 4H_2O$. *J. Am. Chem. Soc.* **113**, 5873.

Chaboussant, G., R. Basler, A. Sieber, S. Ochsenbein *et al.* (2002). Low-energy spin excitations in the molecular magnetic cluster V_{15}. *Europhys. Lett.* **59**, 291.

Chiorescu, I., W. Wernsdorfer, A. Müller, H. Bögge *et al.* (2000). Butterfly hysteresis loop and dissipative spin reversal in the $S = 1/2$, V_{15} molecular complex. *Phys. Rev. Lett.* **84**, 3454.

Choi, J., L. A. W. Sanderson, J. L. Musfeldt, A. Ellern *et al.* (2003). Optical properties of the molecule-based magnet $K_6[V_{15}As_6O_{42}(H_2O)]8H_2O$. *Phys. Rev. B* **68**, 064412.

Cornia, A., M. Affronte, A. G. M. Jansen, D. Gatteschi *et al.* (2000). Magnetic anisotropy of Mn_{12}-acetate nanomagnets from high-field torque magnetometry. *Chem. Phys. Lett.* **322**, 477.

Dearden, A. L., S. Parsons and R. E. P. Winpenny (2001). Synthesis, structure, and preliminary magnetic studies of a Ni_{24} wheel. *Angew. Chem. Int. Ed. Engl.* **40**, 151.

Dressel, M., B. Gorshunov, K. Rajagopal, S. Vongtragool *et al.* (2003). Quantum tunneling and relaxation in Mn_{12}-acetate studied by magnetic spectroscopy. *Phys. Rev. B* **67**, 060405.

Eppley, H. J., H.-L. Tsai, N. de Vries, K. Folting *et al.* (1995). High-spin molecules: Unusual magnetic susceptibility relaxation effects in $[Mn_{12}O_{12}(O_2CEt)_{16}(H_2O)_3]$ (S=9) and the one-electron reduction product $(PPh_4)[Mn_{12}O_{12}(O_2CEt)_{16}(H_2O)_4]$ (S=19/2). *J. Am. Chem. Soc.* **117**, 301.

Ferlay, S., T. Mallah, R. Ouahès, P. Veillet *et al.* (1995). A room-temperature organometallic magnet based on Prussian blue. *Nature* **378**(6558), 701.

Feynman, R. P. (1939). Forces in molecules. *Phys. Rev.* **56**, 340.

FLEUR homepage `http://www.flapw.de`

Friedman, J. R., M. P. Sarachik, J. Tejada and R. Ziolo (1996). Macroscopic measurement of resonant magnetization tunneling in high-spin molecules. *Phys. Rev. Lett.* **76**(20), 3830.

Garg, A. (1993). Topologically quenched tunnel splitting in spin systems without Kramers' degeneracy. *Europhys. Lett.* **22**, 205.

Gaspar, A. B., M. C. Muñoz, N. Moliner, V. Ksenofontov *et al.* (2003). Polymorphism and pressure driven thermal spin crossover phenomenon in $[Fe(abpt)_2(NCX)_2]$ (X=S, and Se): Synthesis, structure and magnetic properties. *Monatsh. Chem.* **134**(2), 285.

Gatteschi, D. and L. Pardi (2003). Spin levels of high nuclearity spin clusters. In C. J. O'Connor, editor, *Research Frontiers in Magnetochemistry*, 67–86. World Scientific, Singapore.

Gatteschi, D., L. Pardi, A. L. Barra, A. Müller *et al.* (1991). Layered magnetic-structure of a metal cluster ion. *Nature (London)* **354**, 463.

Gatteschi, D. and R. Sessoli (2003). Quantum tunneling of magnetization and related phenomena in molecular materials. *Angew. Chem. Int. Ed.* **42**, 268.

Gomes, A. M., M. A. Novak, R. Sessoli, A. Caneschi *et al.* (1998). Specific heat and magnetic relaxation of the quantum nanomagnet Mn_{12}Ac. *Phys. Rev. B* **57**, 5021.

Goodenough, J. B. (1955). Theory of the role of covalence in the perovskite-type manganites [La, M(II)]MnO_3. *Phys. Rev.* **100**, 564.

Goodenough, J. B. (1958). An interpretation of the magnetic properties of the perovskite-type mixed crystals $La_{1-x}Sr_xCoO_{3-x}$. *J. Phys. Chem. Solids* **6**, 287.

Gubanov, V. A. and D. E. Ellis (1980). Magnetic transition-state approach to antiferromagnetic ordering: NiO. *Phys. Rev. Lett.* **44**(24), 1633.

Gunnarsson, O., O. Jepsen and O. K. Andersen (1983). Self-consistent impurity calculations in the atomic-spheres approximation. *Phys. Rev. B* **27**(12), 7144.

Hellmann, H. (1937). *Einführung in die Quantentheorie*. Deuticke, Leipzig.

Holmes, S. M. and G. S. Girolami (1999). Sol-gel synthesis of $KV^{II}[Cr^{III}(CN)_6]\cdot 2H_2O$: A crystalline molecule-based magnet with a magnetic ordering temperature above 100 °C. *J. Am. Chem. Soc.* **121**(23), 5593.

Jackson, K. A. and M. R. Pederson (1990). Accurate forces in a local-orbital approach to the local-density approximation. *Phys. Rev. B* **42**, 3276.

Jansen, H. J. F. (1988). Magnetic anisotropy in density-functional theory. *Phys. Rev. B* **38**, 8022.

Jansen, H. J. F. (1999). Magnetic anisotropy in density-functional theory. *Phys. Rev. B* **59**, 4699.

Junquera, J., Ó. Paz, D. Sánchez-Portal and E. Artacho (2001). Numerical atomic orbitals for linear scaling. *Phys. Rev. B* **64**(23), 235111.

Kahn, O. (1993). *Molecular Magnetism*. John Wiley & Sons, Singapore.

Kanamori, J. (1959). Superexchange interaction and symmetry properties of electron orbitals. *J. Phys. Chem. Solids* **10**, 87.

Katsnelson, M. I., V. V. Dobrovitski and B. N. Harmon (1999). Many-spin interactions and spin excitations in Mn_{12}. *Phys. Rev. B* **59**(10), 6919.

Kortus, J., T. Baruah, N. Bernstein and M. R. Pederson (2002a). Magnetic ordering, electronic structure and magnetic anisotropy energy in the high-spin Mn_{10} single molecule magnet. *Phys. Rev. B* **66**, 092403.

Kortus, J., T. Baruah, M. R. Pederson, S. N. Khanna *et al.* (2002b). Magnetic moment and anisotropy in Fe_nCo_m clusters. *Appl. Phys. Lett.* **80**, 4193.

Kortus, J., C. S. Hellberg and M. R. Pederson (2001a). Hamiltonian of the V_{15} spin system from first-principles density-functional calculations. *Phys. Rev. Lett.* **86**, 3400.

Kortus, J., C. S. Hellberg, M. R. Pederson and S. N. Khanna (2001b). DFT studies of the molecular nanomagnet Fe_8 and the V_{15} spin system. *Eur. Phys. J. D* **16**, 177.

Kortus, J. and M. R. Pederson (2000). Magnetic and vibrational properties of the uniaxial $Fe_{13}O_8$ cluster. *Phys. Rev. B* **62**, 5755.

Kortus, J., M. R. Pederson, T. Baruah, N. Bernstein *et al.* (2002c). Density functional studies of single molecule magnets. *Polyhedron* **22**, 1871.

Ksenofontov, V., A. B. Gaspar, J. A. Real and P. Gütlich (2001a). Pressure-induced spin state conversion in antiferromagnetically coupled Fe(II) dinuclear complexes. *J. Phys. Chem.* **105**(49), 12266.

Ksenofontov, V., H. Spiering, S. Reiman, Y. Garcia *et al.* (2001b). Direct monitoring of spin state in dinuclear iron(II) coordination compounds. *Chem. Phys. Lett.* **348**, 381.

Lascialfari, A., Z. H. Jang, F. Borsa, D. Gatteschi *et al.* (2000). Magnetic and structural properties of an octanuclear Cu(II) S=1/2 mesoscopic ring: Susceptibility and NMR measurements. *Phys. Rev. B* **61**, 6839.

Létard, J.-F., J. A. Real, N. Moliner, A. B. Gaspar *et al.* (1999). Light induced excited pair spin state in an iron (II) binuclear spin-crossover compound. *J. Am. Chem. Soc.* **121**(45), 10630.

Leuenberger, M. N. and D. Loss (2001). Quantum computing in molecular magnets. *Nature* **410**(6830), 789.

Leuenberger, M. N., F. Meier and D. Loss (2003). Quantum spin dynamics in molecular magnets. *Monatsh. Chem.* **134**(2), 217.

Liechtenstein, A. I., V. I. Anisimov and J. Zaanen (1995). Density-functional theory and strong interactions: Orbital ordering in Mott-Hubbard insulators. *Phys. Rev. B* **52**(8), R5467.

Liechtenstein, A. I., M. I. Katsnelson, V. P. Antropov and V. A. Gubanov (1987). Local spin density functional approach to the theory of exchange interactions in ferromagnetic metals and alloys. *J. Magn. Magnet. Mater.* **67**(1), 65.

Liechtenstein, A. I., M. I. Katsnelson and V. A. Gubanov (1984). Exchange interactions and spin-wave stiffness in ferromagnetic metals. *J. Phys. F: Metal Phys.* **14**(7), L125.

Linert, W. and M. Verdaguer, editors (2003). *Molecular Magnets*. Springer-Verlag, Wien. Special Edition of Monatshefte für Chemie/Chemical Monthly, Vol. 134, No. 2.

Lis, T. (1980). Preparation, structure, and magnetic properties of a dodecanuclear mixed-valence manganese carboxylate. *Acta Crystallogr. Soc. B* **36**, 2042.

Louie, S. G., S. Froyen and M. L. Cohen (1982). Nonlinear ionic pseudopotentials in spin-density-functional calculations. *Phys. Rev. B* **26**(4), 1738.

Massobrio, C. and E. Ruiz (2003). Localized orbitals vs. pseudopotential-plane waves basis sets: Performances and accuracy for molecular magnetic systems. *Monatsh. Chem.* **134**(2), 317.

Mertes, K. M., Y. Suzuki, M. P. Sarachik, Y. Paltiel *et al.* (2001). Distribution of tunnel splittings in Mn-12 acetate. *Phys. Rev. Lett.* **87**, 227205.

Mirebeau, I., M. Hennion, H. Casalta, H. Andres *et al.* (1999). Low-energy magnetic excitations of the Mn_{12}-acetate spin cluster observed by neutron scattering. *Phys. Rev. Lett.* **83**, 628.

Molecule-based magnets (2000). Special issue of the *MRS Bulletin* **25** (November).

Müller, A., C. Beugholt, P. Kögerler, H. Bögge *et al.* (2000). $[Mo_{12}O_{30}(\mu_2\text{-}OH)_{10}H_2\{Ni^{II}(H_2O)_3\}_4]$, a highly symmetrical e-Keggin unit capped with four Ni^{II} centers: Synthesis and magnetism. *Inorg. Chem.* **39**(23), 5176.

Müller, A. and J. Döring (1988). A novel heteroclyster with d_3-symmetry containing 21 core atoms – $[As_6^{(III)}V_{15}^{(IV)}O_{42}(H_2O)]^{6-}$. *Angew. Chem., Int. Ed. Engl.* **27**, 1721.

Murrie, M., S. J. Teat, H. Stockli-Evans and H. U. Güdel (2003). Synthesis and characterization of a cobalt(ii) single-molecule magnet. *Angew. Chem., Int. Ed. Engl.* **42**, 4653.

NRLMOL homepage `http://cst-www.nrl.navy.mil/~nrlmol`

Oguchi, T., K. Terakura and A. R. Williams (1983). Band theory of the magnetic interaction in MnO, MnS, and NiO. *Phys. Rev. B* **28**(11), 6443.

Ohkoshi, S.-i. and K. Hashimoto (2002). New magnetic functionalities presented by Prussian Blue analogues. *The Electrochemical Society Interface* **11**(3), 34.

Ordejón, P. (1998). Order-N tight-binding methods for electronic-structure and molecular dynamics. *Computational Materials Science* **12**(3), 157.

Painter, G. S. and D. E. Ellis (1970). Electronic band structure and optical properties of graphite from a variational approach. *Phys. Rev. B* **1**(12), 4747.

Park, K., M. R. Pederson and N. Bernstein (2003). Electronic, magnetic, and vibrational properties of the molecular magnet Mn_4 monomer and dimer. `http://arXiv.org/abs/cond-mat/0307145`.

Park, K., M. R. Pederson and C. S. Hellberg (2003b). Properties of low-lying excited manifolds in the Mn_{12} acetate. `http://arXiv.org/abs/cond-mat/0307707`.

Park, K., M. R. Pederson, S. L. Richardson, N. Aliaga-Alcalde *et al.* (2003c). Density-functional theory calculation of the intermolecular exchange interaction in the magnetic Mn_4 dimer. *Phys. Rev. B* **68**, 020405.

Pederson, M. R., N. Bernstein and J. Kortus (2002a). Fourth-order magnetic anisotropy and tunnel splittings in Mn_{12} from spin-orbit-vibron interactions. *Phys. Rev. Lett.* **89**, 097202.

Pederson, M. R. and K. A. Jackson (1990). Variational mesh for quantum-mechanical simulations. *Phys. Rev. B* **41**, 7453.

Pederson, M. R. and K. A. Jackson (1991). Pseudoenergies for simulations on metallic systems. *Phys. Rev. B* **43**, 7312.

Pederson, M. R. and S. N. Khanna (1999a). Electronic and geometrical structure and magnetic ordering in passivated $Mn_{12}O_{12}$-acetate nanomagnets. *Chem. Phys. Lett.* **307**, 253.

Pederson, M. R. and S. N. Khanna (1999b). Electronic structure and magnetism of $Mn_{12}O_{12}$ clusters. *Phys. Rev. B* **59**, R693.

Pederson, M. R. and S. N. Khanna (1999c). Magnetic anisotropy barrier for spin tunneling in $Mn_{12}O_{12}$ molecules. *Phys. Rev. B* **60**, 9566.

Pederson, M. R., B. M. Klein and J. Q. Broughton (1988). Simulated annealing with floating gaussians – Hellmann-Feynman forces without corrections. *Phys. Rev. B* **38**, 3825.

Pederson, M. R., J. Kortus and S. N. Khanna (2000a). Atomic, electronic and vibrational structure and magnetic anisotropy of $Mn_{12}O_{12}$-acetate nanomagnets. In P. Jena, S. N. Khanna and B. K. Rao, editors, *Cluster and Nanostructure Interfaces*, 159–173. World Scientific Publishing, Singapore.

Pederson, M. R., J. Kortus and S. N. Khanna (2002b). Electronic structure based investigation of magnetism in the Fe_8 molecular magnet. *J. Appl. Phys.* **91**, 7149.

Pederson, M. R. and C. C. Lin (1987). All-electron self-consistent variational method for Wannier-type functions – applications to the silicon crystal. *Phys. Rev. B* **35**, 2273.

Pederson, M. R., A. Y. Liu, T. Baruah, E. Z. Kurmaev *et al.* (2002c). Electronic structure of the molecule-based magnet $Mn[N(CN)_2]_2$ from theory and experiment. *Phys. Rev. B* **66**(1), 014446.

Pederson, M. R., D. V. Porezag, J. Kortus and S. N. Khanna (2000b). Theoretical calculations of magnetic order and anisotropy energies in molecular magnets. *J. Appl. Phys.* **87**, 5487.

Pederson, M. R., D. V. Porezag, J. Kortus and D. C. Patton (2000c). Strategies for massively parallel local-orbital-based electronic structure methods. *phys. stat. sol. (b)* **217**, 197.

Perdew, J. P., K. Burke and M. Ernzerhof (1996). Generalized gradient approximation made simple. *Phys. Rev. Lett.* **77**(18), 3865.

Perdew, J. P., K. Burke and M. Ernzerhof (1997). Erratum: Generalized gradient approximation made simple [Phys. Rev. Lett. 77, 3865 (1996)]. *Phys. Rev. Lett.* **78**(7), 1396.

Pilawa, B., R. Desquiotz, M. T. Kelemen, M. Weickenmeier *et al.* (1997). Magnetic properties of new Fe_6 (triethanolaminate(3-))6 spin-clusters. *J. Magn. Magn. Mater.* **177-181**, 748.

Porezag, D. and M. R. Pederson (1999). Optimization of Gaussian basis sets for density-functional calculations. *Phys. Rev. A* **60**, 2840.

Porezag, D. V. and M. R. Pederson (1996). Infrared intensities and Raman-scattering activities within density-functional theory. *Phys. Rev. B* **54**, 7830.

Postnikov, A. V., S. G. Chiuzbăian, M. Neumann and S. Blügel (2003a). Electron spectroscopy and density-functional study of "ferric wheel" molecules. (to be published in *J. Phys. Chem. Solids*; see `http://arXiv.org/abs/cond-mat/0306430`).

Postnikov, A. V., P. Entel and J. M. Soler (2003b). Density functional simulation of small Fe nanoparticles. *Eur. Phys. J. D* **25**(3), 261.

Postnikov, A. V., J. Kortus and S. Blügel (2003c). Ab initio simulations of Fe-based ferric wheels. *Molecular Physics Reports* **38**, 56. (`http://arXiv.org/abs/cond-mat/0307292`).

Pulay, P. (1969). Ab initio calculation of force constants and equilibrium geometries in polyatomic molecules. I. theory. *Mol. Phys.* **17**, 197.

Quong, A. A., M. R. Pederson and J. L. Feldman (1993). 1st principles determination of the interatomic force-constant tensor of the fullerene molecule. *Sol. Stat. Comm.* **87**, 535.

Rajaraman, G. and R. E. P. Wimpenny, private communication.

Rentschler, E., D. Gatteschi, A. Cornia, A. C. Fabretti *et al.* (1996). Molecule-based magnets: Ferro- and antiferromagnetic interactions in copper(II)-polyorganosiloxanolate clusters. *Inorg. Chem.* **35**, 4427.

Robinson, R. A., P. J. Brown, D. N. Argyriou, D. N. Hendrickson *et al.* (2000). Internal magnetic structure of Mn_{12} acetate by polarized neutron diffraction. *J. Phys.: Condens. Matter* **12**, 2805.

Rosen, A., D. E. Ellis, H. Adachi and F. W. Averill (1976). Calculations of molecular ionization energies using a self-consistent charge Hartree-Fock-Slater method. *Journal of Chemical Physics* **65**(9), 3629.

Saalfrank, R. W., I. Bernt, E. Uller and F. Hampel (1997). Template-mediated self assembly of six- and eight-membered iron coronates. *Angew. Chem. – Intern. Edition* **36**(22), 2482.

Sánchez-Portal, D., E. Artacho and J. M. Soler (1996). Analysis of atomic orbital basis sets from the projection of plane-wave results. *J. Phys.: Condens. Matter* **8**(26), 3859.

Sánchez-Portal, D., P. Ordejón, E. Artacho and J. M. Soler (1997). Density-functional method for very large systems with LCAO basis sets. *Int. J. Quant. Chem.* **65**(5), 453.

Sandratskii, L. M. (1998). Noncollinear magnetism in itinerant-electron systems: theory and applications. *Adv. Phys.* **47**(1), 91.

SIESTA homepage `http://www.uam.es/siesta`

Schneider, G. and H. J. F. Jansen (2000). Role of orbital polarization in calculations of the magnetic anisotropy. *J. Appl. Phys.* **87**, 5875.

Schromm, S., O. Waldmann and P. Müller (2003). . *Phys. Rev. B*, to be published.

Schwarz, K. and P. Mohn (1984). Itinerant metamagnetism in YCO_2. *J. Phys. F: Metal Phys.* **14**(7), L129.

Sessoli, R., H. Tsai, A. Schake, S. Y. Wang *et al.* (1993). High-spin molecules – $[Mn_{12}O_{12}(O_2CR)_{16}(H_2O)_4]$. *J. Am. Chem. Soc.* **115**, 1804.

Shick, A., A. J. Freeman, R. Q. Wu and L. J. Chen (1998). First-principles determinations of magneto-crystalline anisotropy and magnetostriction in bulk and thin-film transition metals. *J. Magnetism and Magnetic Mat.* **177**, 1216.

Soler, J. M., E. Artacho, J. D. Gale, A. García *et al.* (2002). The SIESTA method for *ab initio* order-N materials simulation. *J. Phys.: Condens. Matter* **14**(11), 2745.

Svane, A. and O. Gunnarsson (1988). Localization in the self-interaction-corrected density-functional formalism. *Phys. Rev. B* **37**(16), 9919.

Svane, A. and O. Gunnarsson (1990). Transition-metal oxides in the self-interaction-corrected density-functional formalism. *Phys. Rev. Lett.* **65**(9), 1148.

Taft, K. L., C. D. Delfs, G. C. Papaefthymiou, S. Foner *et al.* (1994). $[Fe(OMe)_2(O_2CCH_2Cl)]_{10}$, a molecular ferric wheel. *J. Am. Chem. Soc.* **116**, 823.

Taft, K. L. and S. J. Lippard (1990). Synthesis and structure of $[Fe(OMe)_2(O_2CCH_2Cl)]_{10}$: a molecular ferric wheel. *J. Am. Chem. Soc.* **112**, 9629 .

TBLMTO homepage `http://www.mpi-stuttgart.mpg.de/andersen/`

Troullier, N. and J. L. Martins (1991). Efficient pseudopotentials for plane-wave calculations. *Phys. Rev. B* **43**(3), 1993.

van Slageren, J., R. Sessoli, D. Gatteschi, A. A. Smith *et al.* (2002). Magnetic anisotropy of the antiferromagnetic ring $[Cr_8Fe_8Piv_{16}]$. *Chem. - Eur. J.* **8**, 277.

van Vleck, J. (1937). On the anisotropy of cubic ferromagnetic crystals. *Phys. Rev.* **52**, 1178.

Verdaguer, M. (2001). Rational synthesis of molecular magnetic materials: a tribute to Olivier Kahn. *Polyhedron* **20**, 1115.

Verdaguer, M., A. Bleuzen, C. Train, R. Garde *et al.* (1999). Room-temperature molecule-based magnets. *Phil. Trans. R. Soc. Lond. A* **357**(1762), 2959.

Verdaguer, M., N. Galvez, R. Garde and C. Desplanches (2002). Electrons at work in Prussian Blue analogues. *The Electrochemical Society Interface* **11**(3), 29.

Waldmann, O., R. Koch, S. Schromm, J. Schülein *et al.* (2001). Magnetic anisotropy of a cyclic octanuclear fe(III) cluster and magneto-structural correlations in molecular ferric wheels. *Inorg. Chem.* **40**, 2986.

Waldmann, O., J. Schülein, R. Koch, P. Müller *et al.* (1999). Magnetic anisotropy of two cyclic hexanuclear Fe(III) clusters entrapping alkaline ions. *Inorganic Chemistry* **38**(25), 5879.

Watton, S. P., P. Fuhrmann, L. E. Pence, A. Caneschi *et al.* (1997). A cyclic octadecairon(III) complex, the molecular 18-wheeler. *Angew. Chem. Int. Ed. Engl.* **36**, 2774.

Wernsdorfer, W., N. Aliaga-Alcalde, D. N. Hendrickson and G. Christou (2002). Exchange-biased quantum tunnelling in a supramolecular dimer of single-molecule magnets. *Nature* **416**(6879), 406.

Wernsdorfer, W., T. Ohm, C. Sangregorio, R. Sessoli *et al.* (1999). Observation of the distribution of molecular spin states by resonant quantum tunneling of the magnetization. *Phys. Rev. Lett.* **82**, 3903.

Wernsdorfer, W. and R. Sessoli (1999). Quantum phase interference and parity effects in magnetic molecular clusters. *Science* **284**, 133.

Wieghardt, K., K. Pohl, I. Jibril and G. Huttner (1984). Hydrolysis products of the monomeric amine complex $(C_6H_{15}N_3)FeCl_3$ - the structure of the octameric iron (III) cation of $[[(C_6H_{15}N_3)_6Fe_8(\mu_3\text{-}O)_2(\mu_2\text{-}OH)_{12}]Br_7(H_2O)]Br{\cdot}8H_2O$. *Angew. Chem., Int. Ed. Engl.* **23**, 77.

Yang, E.-C., D. N. Hendrickson, W. Wernsdorfer, M. Nakano *et al.* (2002). Cobalt single-molecule magnet. *J. Appl. Phys.* **91**(10), 144.

Zeng, Z., D. Guenzburger and D. E. Ellis (1999). Electronic structure, spin couplings, and hyperfine properties of nanoscale molecular magnets. *Phys. Rev. B* **59**(10), 6927.

Zhang, Y. and W. Yang (1998). Comment on "Generalized gradient approximation made simple". *Phys. Rev. Lett.* **80**(4), 890.

Zhong, X. F., W. Y. Ching and W. Lai (1991). Calculation of spin-reorientation temperature in $Nd_2Fe_{14}B$. *J. Appl. Phys.* **70**, 6146.